

# I Bet You Did Not Mean That: Testing Semantic Importance via Betting

Jacopo Teneggi<sup>1,2</sup>  
jtenegg1@jhu.edu

Jeremias Sulam<sup>1,3</sup>  
jsulam1@jhu.edu

<sup>1</sup>Mathematical Institute for Data Science (MINDS), Johns Hopkins University

<sup>2</sup>Department of Computer Science, Johns Hopkins University

<sup>3</sup>Department of Biomedical Engineering, Johns Hopkins University





code: <https://github.com/Sulam-Group/IBYDMT>

demo: <https://huggingface.co/spaces/jacopoteneggi/IBYDMT>

## Abstract

Recent works have extended notions of feature importance to *semantic concepts* that are inherently interpretable to the users interacting with a black-box predictive model. Yet, precise statistical guarantees, such as false positive rate and false discovery rate control, are needed to communicate findings transparently and to avoid unintended consequences in real-world scenarios. In this paper, we formalize the global (i.e., over a population) and local (i.e., for a sample) statistical importance of semantic concepts for the predictions of opaque models by means of conditional independence, which allows for rigorous testing. We use recent ideas of sequential kernelized independence testing (SKIT) to induce a rank of importance across concepts, and showcase the effectiveness and flexibility of our framework on synthetic datasets as well as on image classification tasks using several and diverse vision-language models.

## Which concepts are important for the predictions of a fixed classifier?

<p><u>Prediction:</u> blue jay</p>  <p><u>Concept importance:</u></p> <ul style="list-style-type: none"> <li>blue crown ✓</li> <li>blue forehead ✓</li> <li>blue under tail ✓</li> <li>grey breast ✓</li> <li>grey underparts ✓</li> <li>multi-colored breast ✓</li> <li>red bill ✗</li> <li>white bill ✗</li> <li>pink nape ✗</li> <li>is green ✗</li> <li>is iridescent ✗</li> <li>small ✗</li> <li>pink under tail ✗</li> </ul>	<p><u>Prediction:</u> frigatebird</p>  <p><u>Concept importance:</u></p> <ul style="list-style-type: none"> <li>hooked seabird bill ✓</li> <li>forked tail ✓</li> <li>is black ✓</li> <li>black upper tail ✓</li> <li>black back ✓</li> <li>solid wing ✓</li> <li>solid tail ✓</li> <li>all-purpose bill ✗</li> <li>brown wing ✗</li> <li>pointed tail ✗</li> <li>orange belly ✗</li> <li>striped breast ✗</li> <li>green nape ✗</li> </ul>	<p><u>Prediction:</u> mallard</p>  <p><u>Concept importance:</u></p> <ul style="list-style-type: none"> <li>spatulate bill ✓</li> <li>duck-like ✓</li> <li>olive throat ✓</li> <li>medium ✓</li> <li>yellow bill ✓</li> <li>multi-colored wing ✓</li> <li>red underparts ✗</li> <li>masked head ✗</li> <li>buff leg ✗</li> <li>orange nape ✗</li> <li>long-legged-like ✗</li> <li>rounded tail ✗</li> <li>red breast ✗</li> </ul>	<p><u>Prediction:</u> glossy starling</p>  <p><u>Concept importance:</u></p> <ul style="list-style-type: none"> <li>blue underparts ✓</li> <li>blue upperparts ✓</li> <li>black underparts ✓</li> <li>black breast ✓</li> <li>yellow eye ✓</li> <li>plain head ✓</li> <li>black bill ✓</li> <li>swallow-like ✗</li> <li>iridescent breast ✗</li> <li>brown eye ✗</li> <li>pink eye ✗</li> <li>green leg ✗</li> <li>duck-like ✗</li> </ul>
---	--	---	--

Example results for CLIP-ViT-L/14 on images from the CUB-200-2011 dataset.  
 ✓: important concept, ✗: not important concept.

# Contents

<b>1</b>	<b>Introduction</b>	<b>3</b>
1.1	Summary of Contributions and Related Works . . . . .	4
<b>2</b>	<b>Background</b>	<b>5</b>
<b>3</b>	<b>Testing Semantic Importance via Betting</b>	<b>5</b>
3.1	Defining Statistical Semantic Importance . . . . .	6
3.2	Testing by Betting . . . . .	7
3.3	Testing Global Semantic Importance with SKIT . . . . .	8
3.4	Testing Global Conditional Semantic Importance with c-SKIT . . . . .	10
3.5	Testing Local Conditional Semantic Importance with x-SKIT . . . . .	12
3.6	Controlling False Discovery Rate when Testing Multiple Concepts . . . . .	12
<b>4</b>	<b>Synthetic Experiments</b>	<b>13</b>
4.1	Gaussian Data . . . . .	13
4.2	Counting MNIST Digits . . . . .	16
<b>5</b>	<b>Real-world Experiments</b>	<b>20</b>
5.1	AwA2 Dataset . . . . .	21
5.2	CUB Dataset . . . . .	23
5.3	Imagenette Dataset . . . . .	24
<b>6</b>	<b>Conclusions</b>	<b>26</b>
<b>A</b>	<b>Testing by Betting</b>	<b>33</b>
A.1	Test Martingales . . . . .	33
A.2	Symmetry-based Two-sample Sequential Testing . . . . .	34
A.3	Betting Strategies . . . . .	34
<b>B</b>	<b>Technical Details on Payoff Functions</b>	<b>35</b>
B.1	Computing $\rho_t^{\text{SKIT}}$ . . . . .	36
B.2	Computing $\rho_t^{\text{c-SKIT}}$ . . . . .	37
B.3	Computing $\rho_t^{\text{x-SKIT}}$ . . . . .	38
<b>C</b>	<b>Proofs</b>	<b>38</b>
<b>D</b>	<b>Experimental Details</b>	<b>40</b>
D.1	Estimating Conditional Distributions from Data . . . . .	40
D.2	AwA2 Dataset . . . . .	43
D.3	CUB Dataset . . . . .	45
D.4	Imagenette Dataset . . . . .	47

# 1 Introduction

Providing guarantees on the decision-making processes of autonomous systems, often based on complex black-box machine learning models, is paramount for their safe deployment. This need motivates efforts towards *responsible artificial intelligence*, which broadly entails questions of reliability, robustness, fairness, and interpretability. One popular approach to the latter is to use post-hoc explanation methods to identify the features that contribute the most towards the predictions of a model.<sup>1</sup> Several alternatives have been proposed over the past few years, drawing from various definitions of *features* (e.g., pixels—or groups thereof—for vision tasks [40], words for language tasks [20], or nodes and edges for graph learning [81]) and of *importance* (e.g., gradients for Grad-CAM [55], Shapley values for SHAP [14, 41, 67], or information-theoretic quantities [42]). While most explanation methods highlight important features in the input space of the predictor, users may care more about their meaning. For example, a radiologist may want to know whether a model considered the size and spiculation of a lung nodule to quantify its malignancy, and not just its raw pixel values.

To decouple importance from input features, Kim et al. [33] showed how to learn vector representations of *semantic concepts* that are inherently interpretable to users (e.g., “stripes”, “sky”, or “sand”) and how to study their gradient importance for model predictions. Recent vision-language models that jointly learn an image and text encoder—such as CLIP [15, 49]—have made these representations, commonly referred to as concept activation vectors (CAVs), more easily accessible. With these models, obtaining the vector representation of a concept boils down to a forward pass of the pretrained text encoder, which alleviates the need of a dataset comprising images annotated with their concepts. Several recent works have defined semantic importance—both with CAVs and CLIP embeddings—by means of *concept bottleneck models* (e.g., CBM [35], PCBM [82], LaBo [80]), information-theoretic quantities (e.g., V-IP [36]), sparse coding (e.g., CLIP-IP-OMP [12], SpLiCe [6]), *network dissection* [2] (e.g., CLIP-DISSECT [45], TextSpan [25], INVITE [13]), or causal inference (e.g., DiConStruct [43], Sani et al. [53]).

On the other hand, it is important for notions of interpretability to communicate findings precisely and transparently in order to avoid unintended consequences in downstream decision tasks. Going back to the example of a radiologist diagnosing lung cancer, how should they interpret two concepts with different importance scores? Does their difference in importance carry any statistical meaning? To start addressing similar questions [9, 68] introduced statistical tests for the local (i.e., on a sample) conditional independence structure of a model’s predictions. Framing importance by means of conditional independence allows for rigorous testing with false positive rate control. That is, for a user-defined significance level  $\alpha \in (0, 1)$ , the probability of wrongly deeming a feature important is no greater than  $\alpha$ , which directly conveys the uncertainty in an explanation. Yet these methods consider features as coordinates in the input space, and it is unclear how to extend these ideas to abstract, semantic concepts.

In this work, we formalize semantic importance at three distinct levels of statistical independence with null hypotheses of increasing granularity: (i) marginally over a population (i.e., global importance), (ii) conditionally over a population (i.e., global conditional importance), and (iii) for a sample (i.e., local conditional importance).<sup>2</sup> Each of these notions will allow us to inquire the extent to which the output of a model depends on specific concepts—both over a population and on specific samples—and thus deem them important. Instead of classical (or *offline* [56]) independence testing techniques [5, 9, 10, 27, 28, 66, 83], which are based on  $p$ -values and informally follow the rule “*reject if  $p \leq \alpha$* ”, we propose to use principles of *testing by betting* (or *sequential testing*) [57], which are based on  $e$ -values [73] and follow the “*reject when  $e \geq 1/\alpha$* ” rule. As we will expand on, this choice is motivated by the fact that sequential testing is data-efficient and adaptive to the hardness of the problem—which naturally induces a rank of importance. We will couple principles of conditional randomization testing (CRT) [10] with recent advances in sequential kernelized

<sup>1</sup>A different approach is to build *inherently interpretable models* [52].

<sup>2</sup>We adopt the distinction between *global* and *local* importance as presented in [17].

independence testing (SKIT) [48, 60], and introduce two novel procedures to test for our definitions of semantic importance: the conditional randomization SKIT (c-SKIT) to study global conditional importance, and—following the explanation randomization test (XRT) framework [68]—the explanation randomization SKIT (x-SKIT) to study local conditional importance. We will illustrate the validity of our proposed tests on synthetic datasets, and showcase their flexibility on zero-shot image classification on real-world datasets across several vision-language models, both CLIP- and non-CLIP-based.

## 1.1 Summary of Contributions and Related Works

In this paper, we will rigorously define notions of statistical importance of semantic concepts for the predictions of black-box models via conditional independence—both globally over a population and locally for individual samples. For any set of concepts, and for each level of independence, we introduce novel sequential testing procedures that induce a rank of importance. Before presenting the details of our methodology, we briefly expand on a few distinctive features of our work.

**Explaining nonlinear predictors.** Compared to recent methods based on concept bottleneck models [35, 80, 81], our framework does not require training a surrogate linear classifier because we study the semantic importance structure of any given, potentially nonlinear and randomized model. This distinction is not minor—training concept bottleneck models results on explanations that pertain to the surrogate (linear) model instead of the original (complex, nonlinear) predictor, and these simpler surrogate models typically reduce performance [46, 82]. In contrast, we provide statistical guarantees directly on the original predictor that would be deployed in the wild.

**Flexible choice of concepts.** Furthermore, our framework does not rely on the presence of a large concept bank (but it can use one if it is available). Instead, we allow users to directly specify which concepts they want to test. This feature is important in settings that involve diverse stakeholders. In medicine, for example, there are physicians, patients, model developers, and members of the regulatory agency tasked with auditing the model—each of whom might desire to use different semantics for their explanations. Current explanation methods cannot account for these differences off-the-self.

**Local semantic explanations.** Our framework entails semantic explanations for specific inputs, whereas prior approaches that rely on the weights of a linear model only inform on the global conditional independence structure between concepts and labels. Recently, Shukla et al. [62] set forth ideas of local semantic importance by combining LIME [51] with T-CAV [33]. Our work differs in that it does not apply to images only, it considers formal notions of statistical importance rather than heuristics of gradient importance, and it provides guarantees such as Type I error and false discovery rate (FDR) control.

**Sequential kernelized testing.** Motivated by the statistical properties of kernelized independence tests [60], we will employ the maximum mean discrepancy (MMD) [28] as the test statistic in our proposed procedures. The recent related work in Shaer et al. [56] introduces the sequential version of the conditional randomization test (CRT) [10], dubbed e-CRT because of the use of  $e$ -values. Unlike our work, Shaer et al. [56] employ residuals of a predictor as test statistic, they do so in the context of global tests only, and unrelated to questions of semantic interpretability.



## 2 Background

In this section, we briefly introduce the necessary notation and general background. Throughout this work, we will denote random variables with capital letters, and their realizations with lowercase. For example,  $X \sim P_X$  is a random variable sampled from a distribution  $P_X$ , and  $x$  indicates a particular realization of  $X$ .

**Problem setup.** We consider  $k$ -fold classification problems such that  $(X, Y) \sim P_{XY}$  is a random sample  $X \in \mathcal{X}$  with its one-hot label  $Y \in \{0, 1\}^k$ , and  $(x, y)$  denotes a particular observation. We assume we are given a fixed predictive model, consisting of an encoder  $f : \mathcal{X} \rightarrow \mathbb{R}^d$  and a classifier  $g : \mathbb{R}^d \rightarrow \mathbb{R}^k$  such that  $h = f(x)$  is a  $d$ -dimensional representation of  $x$ , and  $\hat{y}_{k'} = g(h)_{k'} = g(f(x))_{k'}$  is the prediction of the model for a particular class  $k'$  (e.g.,  $\hat{y}_{k'}$  is the output, or score, for class “dog”). Naturally,  $H, \hat{Y}$  denote the random counterparts of  $h$  and  $\hat{y}$ . Although our contributions do not make any assumptions on the performance of the model,  $f$  and  $g$  can be thought of as *good* predictors, e.g. those that approximate the conditional expectation of  $Y$  given  $X$ .

**Concept bottleneck models (CBMs).** Let  $c = [c_1, \dots, c_m] \in \mathbb{R}^{d \times m}$  be a dictionary of  $m$  concepts such that  $\forall j \in [m] := \{1, \dots, m\}$ ,  $c_j \in \mathbb{R}^d$  is the representation of the  $j^{\text{th}}$  concept—either obtained via CAVs [33] or CLIP’s text encoder. Then,  $z = \langle c, h \rangle$  is the projection of the embedding  $h$  onto the concepts  $c$ , and, with appropriate normalization,  $z_j \in [-1, 1]$  is the *amount* of concept  $c_j$  in  $h$ . Intuitively, CBMs project dense representations onto the subspace of interpretable semantic concepts [35], and their performance strongly depends on the size of the dictionary [46]. For example, it is common for  $m$  to be as large as the embedding size (e.g.,  $d = 718$  for CLIP:ViT-L/14).

In this work, instead, we let concepts be user-defined, allowing for cases where  $m \ll d$  (e.g.,  $m = 20$ ). This is by design as (i) the contributions of this paper apply to any set of concepts, and (ii) it has been shown that humans can only gain valuable information if semantic explanations are succinct [50]. However, we remark that the construction of informative concept banks—especially for domain-specific applications—is subject of ongoing complementary research [19, 46, 75, 77, 78].

**Conditional randomization tests.** Recall that two random variables  $A, B$  are conditionally independent if, and only if, given a third random variable  $C$ , it holds that  $P_{A|B,C} = P_{A|C}$  (i.e.,  $A \perp\!\!\!\perp B \mid C$ ). That is,  $B$  does not provide any more information about  $A$  with  $C$  present. Candes et al. [10] introduced the conditional randomization test (CRT), based on the observation that if  $A \perp\!\!\!\perp B \mid C$ , then the triplets  $(A, B, C)$  and  $(A, \tilde{B}, C)$  with  $\tilde{B} \sim P_{B|C}$ , are exchangeable. That is,  $P_{ABC} = P_{A\tilde{B}C}$  and one can essentially *mask*  $B$  without changing the joint distribution. Opposite to classical methods, the CRT assumes the conditional distribution of the covariates is known (i.e.,  $P_{B|C}$ ), which lends itself to settings with ample unlabeled data.

With this general background, we now present the main technical contributions of this paper.

## 3 Testing Semantic Importance via Betting

Our objective is to test the statistical importance of semantic concepts for the predictions of a fixed, potentially nonlinear model, while inducing a rank of importance. Fig. 1 depicts the problem setup—a fixed model, composed of the encoder  $f$  and classifier  $g$ , is probed via a set of concepts  $c$ . This figure also illustrates the key difference with post-hoc concept bottleneck models (PCBMs) [82], in that we do not train a sparse linear layer to approximate  $\mathbb{E}[Y \mid Z]$ . Instead, we focus on characterizing the dependence structure between  $Z$  and  $\hat{Y}$ , i.e. the predictions of the model. Herein, for the sake of conciseness, we will

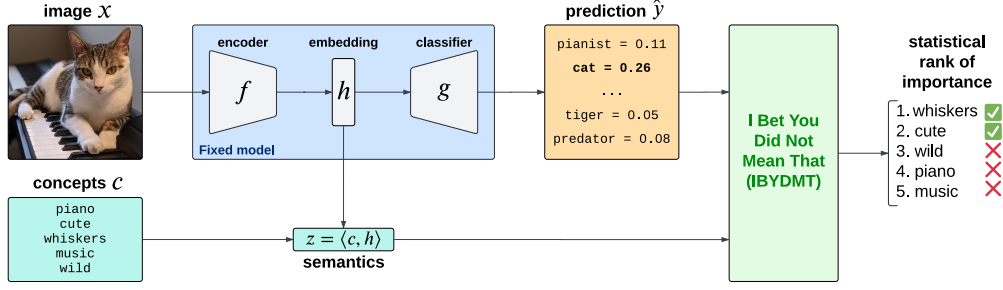


Figure 1: Overview of the problem setup and our contribution.

drop the  $\hat{y}_{k'}$  notation and simply write  $\hat{y}$ ,  $\hat{Y}$  unless unclear from context, and always consider the output of the model for a particular class.

### 3.1 Defining Statistical Semantic Importance

We start by defining *global semantic importance* as marginal dependence between  $\hat{Y}$  and  $Z_j$ ,  $j \in [m]$ .

**Definition 1** (Global semantic importance). For a concept  $j \in [m]$ ,

$$H_{0,j}^G : \hat{Y} \perp\!\!\!\perp Z_j \quad (1)$$

is the global semantic independence null hypothesis.

Rejecting  $H_{0,j}^G$  means that we have observed enough evidence to believe the response of the model depends on concept  $j$ , i.e. concept  $j$  is globally important over the population. Note that both  $\hat{Y}$  and  $Z_j$  are fixed functions of the same random variable  $H$ , i.e.  $\hat{Y} = g(H)$  and  $Z_j = \langle c_j, H \rangle$ .

It is reasonable to wonder whether there is any point in testing  $H_{0,j}^G$  at all—can we obtain two independent random variables from the same one? For example, let  $g$  be a linear classifier such that  $\hat{Y} = \langle w, H \rangle$ ,  $w \in \mathbb{R}^d$ . Intuition might suggest that if  $\langle w, c_j \rangle = 0$  then  $\hat{Y} \perp\!\!\!\perp Z_j$ , i.e. if the classifier is orthogonal to a concept, then the concept cannot be important. We show in the short lemma below (whose proof is in Appendix C.1) that this is false, and that, arguably unsurprisingly, statistical independence is conceptually different from orthogonality between vectors, which motivates the need for our testing procedures.

**Lemma 1.** Let  $\hat{Y} = \langle w, H \rangle$ ,  $w \in \mathbb{R}^d$ . If  $d \geq 3$ , then  $H_{0,j}^G$  is true  $\not\iff \langle w, c_j \rangle = 0$ .

The null hypothesis  $H_{0,j}^G$  above precisely defines the global importance of a concept, but it ignores the information contained in the rest of them, and concepts may be correlated. For example, predictions for class “dog” may be independent of “stick” given “tail” and “paws”, although “stick” is marginally important. To address this, and inspired by the definitions in [10], we introduce *global conditional semantic importance*.

**Definition 2** (Global conditional semantic importance). For a concept  $j \in [m]$ , let  $-j := [m] \setminus \{j\}$  denote all but the  $j^{\text{th}}$  concept. Then,

$$H_{0,j}^{GC} : \hat{Y} \perp\!\!\!\perp Z_j \mid Z_{-j} \quad (2)$$

is the global conditional semantic independence null hypothesis.

Analogous to Definition 1, rejecting  $H_{0,j}^{GC}$  means that we have accumulated enough evidence to believe the response of the model depends on concept  $j$  even in the presence of the remaining concepts, i.e. there is information about  $\hat{Y}$  in concept  $j$  that is missing from the rest.

We stress an important distinction between Definition 2 and PCBM. Recall that PCBM approximates  $\mathbb{E}[Y | Z]$  with a sparse linear layer, which is *inherently interpretable* because the regression coefficients directly inform on the global conditional independence structure of the predictions, i.e. if  $\hat{Y} = \langle \beta, Z \rangle$ ,  $\beta \in \mathbb{R}^m$  then  $\hat{Y} \perp\!\!\!\perp Z_j | Z_{-j} \iff \beta_j = 0$ . In this work, however, we do not assume any parametrization between the concepts and the labels because we want to provide guarantees on the original, fixed classifier  $g$  that acts directly on an embedding  $h$ . From this conditional independence perspective, PCBM can be interpreted as a (parametric) test of true linear independence (i.e.,  $H_{0,j}^{\text{PCBM}} : Y \perp\!\!\!\perp Z_j | Z_{-j}$ ) between the concepts and the labels (note that  $H_{0,j}^{\text{PCBM}}$  has the *true* label  $Y$  and not the prediction  $\hat{Y}$ ), whereas we study the semantic structure of the predictions of a complex model, which may have learned spurious, non-linear correlations of these concepts from data.

Akin to the CRT [10], we assume we can sample from the conditional distribution of the concepts, i.e.  $P_{Z_j | Z_{-j}}$ . Within the scope of this work,  $m$  is small ( $m \approx 20$ ) and we will show how to effectively approximate this distribution with nonparametric methods that do not require prohibitive computational resources. This is an advantage of testing *a few* semantic concepts compared to input features, especially for imaging tasks where the number of pixels is large ( $\gtrsim 10^5$ ) and learning a conditional generative (e.g., a diffusion model) model may be expensive.

Finally, we define the notion of *local conditional semantic importance*. That is, we are interested in finding the most important concepts for the prediction of the model locally on a particular input  $x$ , i.e.  $\hat{y} = g(f(x))$ . Recently, [9, 68] showed how to deploy ideas of conditional randomization testing for local explanations of machine learning models. To summarize, let  $B, C$  be random variables,  $(b, c)$  an observation of  $(B, C)$ , and  $\eta$  a fixed real-valued predictor on  $(b, c)$ . Then, the explanation randomization test (XRT) [68] null hypothesis is  $\eta(b, c) \stackrel{d}{=} \eta(\tilde{B}, c)$ ,  $\tilde{B} \sim P_{B|C=c}$ . That is, the *observed* value of  $B$  does not affect the distribution of the response given the *observed* value of  $C$ . We now generalize these ideas.

**Definition 3** (Local conditional semantic importance). For a fixed  $z \in [-1, 1]^m$  and for any  $C \subseteq [m]$ , denote  $\hat{Y}_C = g(\tilde{H}_C)$  with  $\tilde{H}_C \sim P_{H|Z_C=z_C}$ . Then, for a concept  $j \in [m]$  and a subset  $S \subseteq [m] \setminus \{j\}$ ,

$$H_{0,j,S}^{\text{LC}} : \hat{Y}_{S \cup \{j\}} \stackrel{d}{=} \hat{Y}_S \quad (3)$$

is the local conditional semantic independence null hypothesis.

In words, rejecting  $H_{0,j,S}^{\text{LC}}$  means that, given the observed concepts in  $S$ , concept  $j \notin S$  affects the distribution of the response of the model, hence it is important. For this test, we assume we can sample from the conditional distribution of the embeddings given a subset of concepts (i.e.,  $P_{H|Z_C=z_C}$ ). This is equivalent to solving an inverse problem stochastically, since  $z = \langle c, h \rangle$  and  $c$  is not invertible ( $c \in \mathbb{R}^{d \times m}$ ,  $m \ll d$ ). Hence, there are several embeddings  $h$  that could have generated the observed  $z_C$ . We will use nonparametric sampling ideas to achieve this, stressing that it suffices to sample the embeddings  $H$  and not an entire input image  $X$  since the classifier  $g$  directly acts on  $h$  and the encoder  $f$  is deterministic. Finally, we remark that  $H_{0,j,S}^{\text{LC}}$  differs from the XRT null hypothesis in that conditioning is performed in the space of semantic concepts instead of that of the input.

With these precise notions of semantic importance, we now show how to test for each one of them with principles of sequential kernelized independence testing (SKIT) [48].

## 3.2 Testing by Betting

A classical approach to hypothesis testing consists of formulating a null hypothesis  $H_0$ , collecting data, and then summarizing evidence by means of a  $p$ -value. Under the null, the probability of observing a small

$p$ -value is small.<sup>3</sup> Thus, for a significance level  $\alpha \in (0, 1)$ , we can reject  $H_0$  if  $p \leq \alpha$ . In this setting, all data is collected first, and then processed later (i.e., offline).

Alternatively, one can instantiate a game between a bettor and nature [57, 58]. At each turn of the game, the bettor places a wager against  $H_0$ , and then nature reveals the truth. If the bettor wins, they will increase their wealth, otherwise lose some. More formally, and as is commonly done [48, 56, 60], we define a wealth process  $\{K_t\}_{t \in \mathbb{N}_0}$  with

$$K_0 = 1 \quad \text{and} \quad K_t = K_{t-1} \cdot (1 + v_t \kappa_t) \quad (4)$$

where  $v_t \in [-1, 1]$  is a betting fraction, and  $\kappa_t \in [-1, 1]$  is the payoff of the bet. It is now easy to see that when  $v_t \kappa_t \geq 0$  (i.e., the bettor wins) the wealth increases, and the opposite otherwise.

We briefly include here a condition under which the payoff  $\kappa_t$  guarantees the game is *fair* (under the null, the bettor cannot accumulate wealth and outwin nature) and we can thus use the wealth process to reject  $H_0$  with Type I error control. In particular, for a significance level  $\alpha \in (0, 1)$ , we denote  $\tau = \min\{t \geq 1 : K_t \geq 1/\alpha\}$  the *rejection time* of  $H_0$ .

**Lemma 2** (See Shaer et al. [56], Shekhar and Ramdas [60]). *If*

$$\mathbb{E}_{H_0}[\kappa_t \mid \mathcal{F}_{t-1}] = 0, \quad (5)$$

*where  $\mathcal{F}_{t-1}$  denotes the filtration (i.e., the smallest  $\sigma$ -algebra) of all previous observations, then the wealth process describes a fair game and*

$$\mathbb{P}_{H_0}[\exists t \geq 1 : K_t \geq 1/\alpha] \leq \alpha. \quad (6)$$

The proof of this lemma is included in Appendix A.1 for completeness. The choice of using sequential testing instead of classical offline methods is motivated by two fundamental properties. First, sequential tests are *adaptive* to the hardness of the problem, sometimes provably [60, Proposition 3]. That is, the harder it is to reject the null, the longer the test will take, and vice versa. This naturally induces a rank of importance across concepts—if concept  $c_j$  rejects faster than  $c_{j'}$ , then it is more important (i.e., it is easier to reject the null hypothesis that the predictions do not depend on  $c_j$ ). We stress that this is not always possible by means of  $p$ -values because they do not measure effect sizes: consider two concepts that reject their respective nulls at the same significance level; it is not possible to distinguish which—if any—is more important. As we will show in our experiments, all tests used in this work are adaptive in practice, but statistical guarantees on their rejection times are currently open questions, and we consider them as future work. Second, sequential tests are *sample-efficient* because they do not require analyzing an entire dataset, but only what is needed to reject. This is especially important for conditional randomization tests, where sampling from the conditional may be expensive. In the offline scenario, we would have to resample the entire dataset  $r$  times (and  $r$  is usually of the order of  $10^2$ ), whereas the sequential test would terminate in at most the size of the dataset, providing a speedup of factor  $r$ .<sup>4</sup>

### 3.3 Testing Global Semantic Importance with SKIT

Podkopaev et al. [48] show how to design sequential kernelized tests of independence (i.e.,  $H_0 : A \perp\!\!\!\perp B$ ) by framing them as particular two-sample tests of the form  $H_0 : P = \tilde{P}$ , with  $P = P_{AB}$  and  $\tilde{P} = P_A \times P_B$ . Similarly to [56, 60], they propose to leverage a simple yet powerful observation about the *symmetry* of the data under  $H_0$  [48, Section 4]. We state here the main result we will use in this paper (the proof is included in Appendix A.2).

<sup>3</sup>Recall that a random variable  $p$  is a valid  $p$ -value if  $\mathbb{P}_{H_0}[p \leq \alpha] \leq \alpha, \forall \alpha \in (0, 1)$ .

<sup>4</sup>We note recent connections by Fischer and Ramdas [23] between permutation tests and  $e$ -values.

---

**Algorithm 1** Level- $\alpha$  SKIT for the global importance of concept  $j$ 


---

**Input:** Stream  $(\hat{Y}^{(t)}, Z_j^{(t)}) \sim P_{\hat{Y}Z_j}$ .

```

1:  $K_0 \leftarrow 1$ 
2: Initialize ONS strategy as in Algorithm A.1.
3: for  $t = 1, \dots$  do
4:   Compute  $\rho_t^{\text{SKIT}}$  as in Eq. (11)
5:   Observe  $D^{(2t-1)} = (\hat{Y}^{(2t-1)}, Z_j^{(2t-1)})$  and  $D^{(2t)} = (\hat{Y}^{(2t)}, Z_j^{(2t)})$ 
6:    $\tilde{D}^{(2t-1)} \leftarrow (\hat{Y}^{(2t-1)}, Z_j^{(2t)})$  and  $\tilde{D}^{(2t)} \leftarrow (\hat{Y}^{(2t)}, Z_j^{(2t-1)})$ 
7:   Compute  $\kappa_t^{\text{SKIT}}$  as in Eq. (12)
8:    $K_t \leftarrow K_{t-1} \cdot (1 + v_t \kappa_t)$ 
9:   if  $K_t \geq 1/\alpha$  then
10:    return  $t$ 
11:   end if
12:    $v_{t+1} \leftarrow$  ONS step
13: end for

```

---

**Lemma 3** (See [48, 56, 60]).  $\forall t \geq 1$ , let  $X \sim P$  and  $\tilde{X} \sim \tilde{P}$ , and let  $\rho_t : \mathcal{X} \rightarrow \mathbb{R}$  be any fixed function. Then,

$$\kappa_t = \tanh(\rho_t(X) - \rho_t(\tilde{X})) \quad (7)$$

satisfies Lemma 2 for  $H_0 : P = \tilde{P}$ , i.e. it provides a fair game.

That is, Lemma 3 prescribes how to construct valid payoffs for two-samples tests, and, consequently, tests of independence. We note that the choice of  $\tanh$  provides  $\kappa_t \in [-1, 1]$ , but any arbitrary anti-symmetric function can be used (e.g.,  $\text{sign}$ ). Furthermore, any fixed function  $\rho_t$  is valid but, in general, this function should have a positive value under the alternative in order for the bettor to increase their wealth and the testing procedure to have good power.

In this work, note that the global semantic importance null hypothesis  $H_{0,j}^G$  in Definition 1 can be directly rewritten as a two-sample test, i.e.

$$H_{0,j}^G : \hat{Y} \perp\!\!\!\perp Z_j \quad \text{is equivalent to} \quad H_{0,j}^G : P_{\hat{Y}Z_j} = P_{\hat{Y}} \times P_{Z_j}. \quad (8)$$

In particular, we follow [48] and use the maximum mean discrepancy (MMD) [28] to measure the distance between the joint and product of marginals. In particular, let  $\mathcal{R}_{\hat{Y}}, \mathcal{R}_{Z_j}$  be two reproducing kernel Hilbert spaces (RKHSs) on the domains of  $\hat{Y}$  and  $Z_j$ , respectively (recall that  $\hat{Y}$  and  $Z_j$  are both univariate). Then,  $\rho_t^{\text{SKIT}}$  is the plug-in estimate of  $\text{MMD}(P_{\hat{Y}Z_j}, P_{\hat{Y}} \times P_{Z_j})$  at time  $t$ .<sup>5</sup> Note that, in practice, we only have access to samples from the test distribution  $P_{\hat{Y}Z_j}$  (i.e., the joint) and we employ a permutation approach swapping elements of two consecutive samples to simulate data from the null distribution  $P_{\hat{Y}} \times P_{Z_j}$ .

More formally, let

$$D^{(2t)} = (\hat{Y}^{(2t)}, Z_j^{(2t)}) \sim P_{\hat{Y}Z_j}, \quad \tilde{D}^{(2t-1)} = (\hat{Y}^{(2t-1)}, Z_j^{(2t-1)}) \sim P_{\hat{Y}Z_j} \quad (9)$$

such that

$$\tilde{D}^{(2t)} = (\hat{Y}^{(2t)}, Z_j^{(2t-1)}), \quad \tilde{D}^{(2t-1)} = (\hat{Y}^{(2t-1)}, Z_j^{(2t)}). \quad (10)$$

---

<sup>5</sup>Recall that  $\text{MMD}(P_{AB}, P_A \times P_B)$  is the Hilbert-Schmidt Independence Criterion (HSIC), see Gretton et al. [27].

---

**Algorithm 2** Level- $\alpha$  c-SKIT for the global conditional importance of concept  $j$ 


---

**Input:** Stream  $(\hat{Y}^{(t)}, Z_j^{(t)}, Z_{-j}^{(t)}) \sim P_{\hat{Y}Z_jZ_{-j}}$ .

```

1:  $K_0 \leftarrow 1$ 
2: Initialize ONS strategy (Algorithm A.1)
3: for  $t = 1, \dots$  do
4:   Compute  $\rho_t^{\text{c-SKIT}}$  as in Eq. (14)
5:   Observe  $(\hat{Y}^{(t)}, Z_j^{(t)}, Z_{-j}^{(t)})$ 
6:   Sample  $\tilde{Z}_j^{(t)} \sim P_{Z_j|Z_{-j}=Z_{-j}^{(t)}}$ 
7:   Compute  $k_t^{\text{c-SKIT}}$  as in Eq. (15)
8:    $K_t \leftarrow K_{t-1} \cdot (1 + v_t \kappa_t)$ 
9:   if  $K_t \geq 1/\alpha$  then
10:    return  $t$ 
11:   end if
12:    $v_{t+1} \leftarrow$  ONS step
13: end for

```

---

Then,

$$\rho_t^{\text{SKIT}} := \hat{\mu}_{\hat{Y}Z_j}^{(2(t-1))} - \hat{\mu}_{\hat{Y}}^{(2(t-1))} \otimes \hat{\mu}_{Z_j}^{(2(t-1))} \quad (11)$$

where  $\hat{\mu}_{\hat{Y}Z_j}, \hat{\mu}_{\hat{Y}}, \hat{\mu}_{Z_j}$  are the *mean embeddings* of  $P_{\hat{Y}Z_j}, P_{\hat{Y}}, P_{Z_j}$  in  $\mathcal{R}_{\hat{Y}} \otimes \mathcal{R}_{Z_j}, \mathcal{R}_{\hat{Y}},$  and  $\mathcal{R}_{Z_j}$ , respectively, and  $\otimes$  is the tensor product as in Gretton et al. [28]. We remark that  $\rho_t^{\text{SKIT}}$  is a real-valued operator, i.e.  $\rho_t^{\text{SKIT}} : \mathbb{R} \times \mathbb{R} \rightarrow \mathbb{R}$ , and we include technical details on how to compute it in Appendix B.1. Finally, we note that for all tests presented in this work, we use data up to  $t - 1$  to compute  $\rho_t$  in order to maintain validity of the test, i.e.  $\rho_t$  is fixed conditionally on previous observations. Then, following Lemma 3, we conclude

$$\kappa_t^{\text{SKIT}} := \tanh \left( \rho_t^{\text{SKIT}}(D^{(2t-1)}) + \rho_t^{\text{SKIT}}(D^{(2t)}) - \rho_t^{\text{SKIT}}(\tilde{D}^{(2t-1)}) - \rho_t^{\text{SKIT}}(\tilde{D}^{(2t)}) \right) \quad (12)$$

and Algorithm 1 summarizes the SKIT procedure for the global semantic importance null hypothesis  $H_{0,j}^G$  in Definition 1.

**Computational complexity of SKIT.** Analogous to the original presentation in Shekhar and Ramdas [60], the computational complexity of Algorithm 1 is  $\mathcal{O}(\tau^2)$ , where  $\tau$  is the random rejection time.

We now move on to presenting two novel testing procedures:

1. The conditional randomization SKIT (c-SKIT) for  $H_{0,j}^{\text{GC}}$  in Definition 2, and
2. The explanation randomization SKIT (x-SKIT) for  $H_{0,j,S}^{\text{LC}}$  in Definition 3.

### 3.4 Testing Global Conditional Semantic Importance with c-SKIT

Analogous to the discussion in the previous section, we rephrase the global conditional null hypothesis  $H_{0,j}^{\text{GC}}$  in Definition 2 as a two sample test, i.e.

$$H_{0,j}^{\text{GC}} : \hat{Y} \perp\!\!\!\perp Z_j \mid Z_{-j} \quad \text{is equivalent to} \quad H_{0,j}^{\text{GC}} : P_{\hat{Y}Z_jZ_{-j}} = P_{\hat{Y}\tilde{Z}_jZ_{-j}}, \tilde{Z}_j \sim P_{Z_j|Z_{-j}}. \quad (13)$$



---

**Algorithm 3** Level- $\alpha$  x-SKIT for the local conditional importance of concept  $j$ 

---

**Input:** Observation  $z$ , subset  $S \subseteq [m] \setminus \{j\}$ .

```
1:  $K_0 \leftarrow 1$ 
2: Initialize ONS strategy (Algorithm A.1)
3: for  $t = 1, \dots$  do
4:   Compute  $\rho_t^{\text{x-SKIT}}$  as in Eq. (16)
5:   Sample  $\tilde{H}_{S \cup \{j\}}^{(t)} \sim P_{H|Z_{S \cup \{j\}}=z_{S \cup \{j\}}}$ 
6:   Sample  $\tilde{H}_S^{(t)} \sim P_{H|Z_S=z_S}$ 
7:    $\hat{Y}_{S \cup \{j\}}^{(t)} \leftarrow g(\tilde{H}_{S \cup \{j\}}^{(t)})$ ,  $\hat{Y}_S^{(t)} \leftarrow g(\tilde{H}_S^{(t)})$ 
8:    $\kappa_t \leftarrow \tanh(\rho_t(\hat{Y}_{S \cup \{j\}}^{(t)}) - \rho_t(\hat{Y}_S^{(t)}))$ 
9:    $K_t \leftarrow K_{t-1} \cdot (1 + v_t \kappa_t)$ 
10:  if  $K_t \geq 1/\alpha$  then
11:    return  $t$ 
12:  end if
13:   $v_{t+1} \leftarrow$  ONS step
14: end for
```

---

In contrast with other kernel-based notions of distance between conditional distributions [47, 61, 64]—and akin to the CRT [10]—we assume we can sample from  $P_{Z_j|Z_{-j}}$ , which allows us to directly estimate  $\text{MMD}(P_{\hat{Y}Z_jZ_{-j}}, P_{\hat{Y}\tilde{Z}_jZ_{-j}})$  in our testing procedure (we will expand on how to sample from this distribution shortly). In particular, let  $\mathcal{R}_{\hat{Y}}, \mathcal{R}_{Z_j}, \mathcal{R}_{Z_{-j}}$  be three RKHSs on the domains of  $\hat{Y}, Z_j$ , and  $Z_{-j}$  (i.e.,  $\mathbb{R}, \mathbb{R}, \mathbb{R}^{m-1}$ , where  $m$  is the number of concepts), then, at time  $t$ , the c-SKIT payoff function is

$$\rho_t^{\text{c-SKIT}} := \hat{\mu}_{\hat{Y}Z_jZ_{-j}}^{(t-1)} - \hat{\mu}_{\hat{Y}\tilde{Z}_jZ_{-j}}^{(t-1)}, \quad (14)$$

where  $\hat{\mu}_{\hat{Y}Z_jZ_{-j}}^{(t-1)}, \hat{\mu}_{\hat{Y}\tilde{Z}_jZ_{-j}}^{(t-1)}$  are the mean embeddings of their respective distributions in  $\mathcal{R}_{\hat{Y}} \otimes \mathcal{R}_{Z_j} \otimes \mathcal{R}_{Z_{-j}}$ , and

$$\kappa_t^{\text{c-SKIT}} := \tanh(\rho_t^{\text{c-SKIT}}(\hat{Y}^{(t)}, Z_j^{(t)}, Z_{-j}^{(t)}) - \rho_t^{\text{c-SKIT}}(\hat{Y}^{(t)}, \tilde{Z}_j^{(t)}, Z_{-j}^{(t)})). \quad (15)$$

As before,  $\rho_t^{\text{c-SKIT}}$  is a real-valued operator on  $\mathbb{R} \times \mathbb{R} \times \mathbb{R}^{m-1}$ , and we include the remaining technical details in Appendix B.2. Algorithm 2 summarizes the c-SKIT procedure, which provides Type I error control for  $H_{0,j}^{\text{GC}}$ , as we briefly state in the following proposition (see Appendix C.2 for the proof).

**Proposition 1** (Validity of c-SKIT).  $\forall t \geq 1$ ,  $\kappa_t^{\text{c-SKIT}}$  provides a fair game for  $H_{0,j}^{\text{GC}}$ .

**Computational complexity of c-SKIT.** First note that  $Z_{-j}$  is an  $(m-1)$ -dimensional vector (where  $m$  is the number of concepts). So, at each step of the test, the evaluation of the kernel associated with  $\mathcal{R}_{Z_{-j}}$  requires an additional sum over  $\mathcal{O}(m)$  terms. Furthermore, c-SKIT needs access to a sampler  $P_{Z|Z_{-j}}$ , and we conclude that the computational complexity of Algorithm 2 is  $\mathcal{O}(T_n m \tau^2)$ , where  $T_n$  represents the cost of the sampler on  $n$  samples, and it depends on implementation. For example, in the following, we will use non-parametric samplers with  $T_n = \tau n^2$  since at each step of the test we need to estimate a different conditional probability distribution. Other choices of samplers, such as variational-autoencoders, may not depend on  $\tau$  (they are trained once and only used for inference).

### 3.5 Testing Local Conditional Semantic Importance with x-SKIT

Attentive readers will have noticed that the local conditional semantic null hypothesis  $H_{0,j,S}^{\text{LC}}$  in Definition 3 is already a two-sample test where the test statistic  $P$  is the distribution of the response of the model *with* the observed amount of concept  $j$  (i.e.,  $\hat{Y}_{S \cup \{j\}} = g(\tilde{H}_{S \cup \{j\}})$ ), and the null distribution  $\tilde{P}$  *without* (i.e.,  $\hat{Y}_S = g(\tilde{H}_S)$ ). Herein, we assume we can sample from  $\tilde{H}_C \sim P_{H|Z_C=z_C}$  for any subset  $C \subseteq [m]$ , i.e. the conditional distribution of dense embeddings with specific concepts, which we will address via nonparametric methods in the following section. Then, for an RKHS  $\mathcal{R}_{\hat{Y}}$ , the x-SKIT payoff function is

$$\rho_t^{\text{x-SKIT}} := \hat{\mu}_{\hat{Y}_{S \cup \{j\}}}^{(t-1)} - \hat{\mu}_{\hat{Y}_S}^{(t-1)} \quad (16)$$

with  $\hat{\mu}_{\hat{Y}_{S \cup \{j\}}}^{(t-1)}, \hat{\mu}_{\hat{Y}_S}^{(t-1)}$  mean embeddings of the distributions in  $\mathcal{R}_{\hat{Y}}$ , and

$$\kappa_t^{\text{x-SKIT}} := \tanh(\rho_t^{\text{x-SKIT}}(\hat{Y}_{S \cup \{j\}}) - \rho_t^{\text{x-SKIT}}(\hat{Y}_S)). \quad (17)$$

That is,  $\rho_t^{\text{x-SKIT}}$  is the plug-in estimate of  $\text{MMD}(\hat{Y}_{S \cup \{j\}}, \hat{Y}_S)$  and, analogous to above, we include technical details in Appendix B.3. Then, the x-SKIT testing procedure (which is summarized in Algorithm 3) provides Type I error control for  $H_{0,j,S}^{\text{LC}}$ , as the following proposition summarizes (the proof is included in Appendix C.3).

**Proposition 2** (Validity of x-SKIT).  $\forall t \geq 1$ ,  $\kappa_t^{\text{x-SKIT}}$  provides a fair game for  $H_{0,j,S}^{\text{LC}}$ .

**Computational complexity of x-SKIT.** Note that Algorithm 3 assumes access to a sampler  $P_{H|Z_C=z_C}$ , so its computational complexity is  $\mathcal{O}(T_n \tau^2)$ , where, similarly to above,  $T_n$  is the cost of the sampler. We briefly remark that, for the nonparametric samplers used in this work,  $T_n = n^2$  (compared to  $\tau n^2$  for c-SKIT) because we only need to estimate one conditional distribution.

### 3.6 Controlling False Discovery Rate when Testing Multiple Concepts

So far, we have introduced our tests and discussed their statistical validity for *one concept at a time*. However, in practice, we are interested in testing  $m \geq 1$  concepts, and it is well-known that multiple hypothesis testing requires appropriate corrections to avoid inflated significance levels. Here, we use a result of Wang and Ramdas [76] to devise a greedy post-processing algorithm that guarantees false discovery rate (FDR) control [3] and provides a rank of importance. In particular, given  $m$  null hypotheses  $H_0^{(1)}, \dots, H_0^{(m)}$ , denote  $e^{(1)}, \dots, e^{(m)}$  their respective  $e$ -values and let  $\mathcal{E} : [0, \infty]^m \rightarrow 2^{[m]}$  be an  $e$ -testing procedure such that  $\tilde{S} = \mathcal{E}(e^{(1)}, \dots, e^{(m)})$  is the set of rejected null hypotheses. Then, FDR is defined as the expected proportion of false discoveries to the number of total findings, i.e.

$$\text{FDR} := \mathbb{E} \left[ \frac{|\tilde{S} \cap S_0|}{|\tilde{S}|} \right], \quad (18)$$

where  $S_0 := \{j \in [m] : H_0^{(j)} \text{ is true}\}$  is the set of true null hypotheses (i.e., the ones that should not be rejected). Following [7, 76], we say that  $\mathcal{E}$  is *self-consistent at level  $\alpha$*  if every rejected  $e$ -value satisfies  $e^{(j)} \geq m/\alpha|\tilde{S}|$ , and we now state the lemma we use to construct our post-processor (see Algorithm 4).

**Lemma 4** (See Wang and Ramdas [76]). *Any self-consistent  $e$ -testing procedure at level  $\alpha$  controls FDR at level  $\alpha$  for arbitrary configurations of  $e$ -values.*

---

**Algorithm 4** Greedy FDR post-processor.

---

**Input:** Wealth processes  $\{K_t^{(i)}\}, \dots, \{K_t^{(m)}\}, t \in \mathbb{N}_0$ , significance level  $\alpha$ .

```
1:  $\tilde{S} \leftarrow \emptyset$ 
2: for  $s = 1, \dots, m$  do
3:    $j', \tau' \leftarrow \arg \min_{j \in [m] \setminus \tilde{S}, \tau \in [0, \infty]} \tau$  s.t.  $K_\tau^{(j)} \geq m/\alpha s$ 
4:   if  $\tau' = \infty$  then
5:     return  $\tilde{S}$ 
6:   end if
7:    $\tilde{S} \leftarrow \tilde{S} \cup \{j'\}$ 
8: end for
9: return  $\tilde{S}$ 
```

---

Recall that the optional stopping theorem implies that for a test martingale  $\{K_t\}_{t \in \mathbb{N}_0}$ , the wealth  $K_t$  is an  $e$ -value for any  $t \geq 1$ . Then, intuitively, Algorithm 4 transforms an  $e$ -testing procedure  $\mathcal{E}$  into a self-consistent one by greedily rejecting concepts as soon as they cross the adjusted threshold  $m/\alpha|\tilde{S}|$ . Note that we do not know the number of rejections *a priori*, and that  $m/\alpha|\tilde{S}|$  is a decreasing function of  $|\tilde{S}|$ . Hence, the adjusted threshold for the first rejected concept will be  $m/\alpha$  (which matches the common Bonferroni correction [8]),  $m/2\alpha$  for the second one, then  $m/3\alpha$ , and so on and so forth. The procedure stops when no more concepts reach the threshold, and concepts are sorted by their adjusted rejection times. We remark that Algorithm 4 runs in  $\mathcal{O}(m)$  time, and that it does not change the individual testing procedures. This is important because, in practice, concepts are first tested concurrently, and then post-processed.

## 4 Synthetic Experiments

In this section, we showcase the main properties of our tests of two synthetic datasets.<sup>6</sup> Readers who prefer to focus on real-world applications may skip ahead to Section 5.

### 4.1 Gaussian Data

We start by illustrating all sequential tests presented in this work are valid, and that they adapt to the hardness of the problem, i.e. the weaker the dependence structure, the longer their rejection times. We devise a synthetic dataset with a nonlinear response such that all distributions are known and we can sample from the exact conditional distribution.

The data-generating process we consider is defined as

$$Z_1 \sim \mathcal{N}(\mu_1, \sigma_1^2) \quad \mu_1 = 1, \sigma_1 = 1 \quad (19)$$

$$Z_2 \sim \mathcal{N}(\mu_2, \sigma_2^2) \quad \mu_2 = -1, \sigma_2 = 1 \quad (20)$$

$$Z_3 \mid Z_1 \sim \mathcal{N}(Z_1, \sigma_3^2) \quad \sigma_3 = 1 \quad (21)$$

and

$$Y \mid Z \sim S(\beta_1 Z_1 + \beta_2 Z_2 Z_3 + \beta_3 Z_3) + \epsilon, \quad (22)$$

where  $S$  is the sigmoid function,  $\epsilon \sim \mathcal{N}(0, \sigma_0^2)$ ,  $\sigma_0 = 0.01$  is independent Gaussian noise, and  $\beta_i, i = 1, 2, 3$  are coefficients that will allow us to test different conditions. Then, it follows that

$$g(z) = \mathbb{E}[Y \mid Z = z] = S(\beta_1 z_1 + \beta_2 z_2 z_3 + \beta_3 z_3) \quad (23)$$

---

<sup>6</sup>Code to reproduce experiments is available at <https://github.com/Sulam-Group/IBYDMT>.

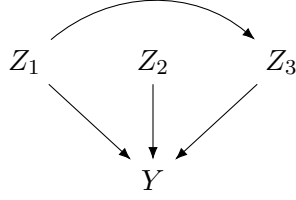


Figure 2: Pictorial representation of the data-generating process for the synthetic dataset.

and

$$Z_1 \mid Z_3 \sim \mathcal{N} \left( \frac{\sigma_1^2}{\sigma_1^2 + \sigma_3^2} Z_3 + \frac{\sigma_3^2}{\sigma_1^2 + \sigma_3^2} \mu_1, \left( \frac{1}{\sigma_1^2} + \frac{1}{\sigma_3^2} \right)^{-1} \right). \quad (24)$$

Fig. 2 depicts the data-generating process. We remark that, for this experiment, we assume there exists a known parametric relation between the response  $Y$  and the *concepts*  $Z$ . This is only to verify our tests retrieve the ground-truth structure, and our contributions do not rely on this assumption. With this data-generating process, it holds that:

1. If  $\beta_2 = 0$  then  $Y \perp\!\!\!\perp Z_2$ ,
2. If  $\beta_1 = 0$  then  $Y \perp\!\!\!\perp Z_1 \mid Z_{-1}$ , and
3. For an observation  $Z = z$ , if  $z_3 = 0$  then  $g(\tilde{Z}_{\{2,3\}}) \stackrel{d}{=} g(\tilde{Z}_3)$  with  $\tilde{Z}_C \sim P_{Z|Z_C=z_C}$ .

We test each condition with SKIT, c-SKIT, and x-SKIT, respectively. We use both a linear and RBF kernel with bandwidth set to the median pairwise distance between all previous observations (commonly referred to as the *median heuristic* [26]). For each test, we estimate the *rejection rate* (i.e., how often a test rejects), and the *expected rejection time* (i.e., how many steps of the test it takes to reject) over 100 draws of  $\tau^{\max} = 1000$  samples, and with a significance level  $\alpha = 0.05$ . We remark that a normalized rejection time of 1 means failing to reject in at most  $\tau^{\max}$  steps.

#### 4.1.1 Global Importance with SKIT

First, we test that

$$\beta_2 = 0 \implies Y \perp\!\!\!\perp Z_2 \quad (25)$$

with the symmetry-based SKIT test in Algorithm 1. Fig. 3a shows samples from the joint distribution  $P_{Y Z_2}$  for  $\beta_2 = 1$  and  $\beta_2 = 0$ . As expected, when  $\beta_2 = 0$ , the slope of the linear regression (red dashed line) is  $\approx 0$  because  $Y$  and  $Z_2$  are independent. Fig. 3b reports average rejection rate and average rejection time as a function of  $\beta_2$ . As  $\beta_2$  increases, the strength of the dependency between  $Y$  and  $Z_2$  increases, and the rejection time decreases—this adaptive behavior is characteristic of sequential tests.

We can verify that the rejection rate is below the significance level  $\alpha = 0.05$  when  $\beta_2 = 0$ , and that the SKIT procedure provides Type I error control. Finally, we note that both kernels perform similarly for this test, with the linear kernel generally rejecting less than the RBF one, and with longer rejection times.

#### 4.1.2 Global Conditional Importance with c-SKIT

Then, we test that

$$\beta_1 = 0 \implies Y \perp\!\!\!\perp Z_1 \mid Z_{-1} \quad (26)$$

with c-SKIT (Algorithm 2). We remark that we can sample from the exact conditional distribution  $P_{Z_1|Z_{-1}} = P_{Z_1|Z_{\{2,3\}}}$  because  $Z_2$  is independent of  $Z_1$  by construction, and the conditional  $P_{Z_1|Z_3}$  can be computed

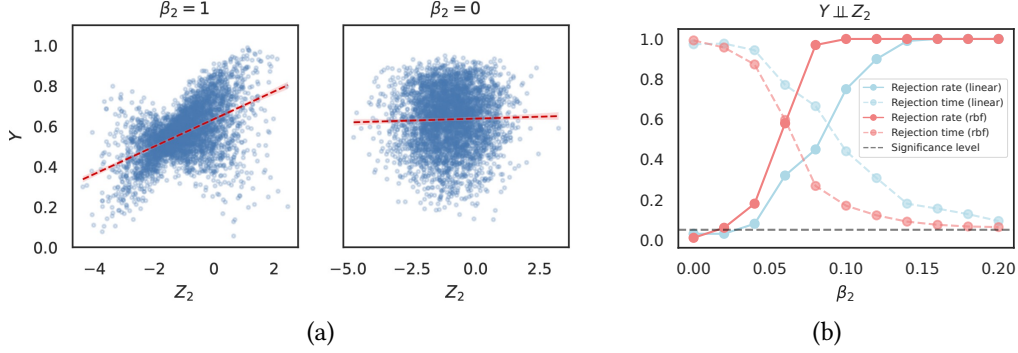


Figure 3: Global importance results for  $H_0 : Y \perp Z_2$  with SKIT. (a) Marginal distributions of  $Y$  and  $Z_2$  for  $\beta_2 = 1$  and  $0$ , respectively. The red dashed line is the linear regression between the two variables, and, as expected, the slope is  $\approx 0$  for  $\beta_2 = 0$ . (b) Mean rejection rate and mean rejection time for SKIT with a linear and RBF kernel, as a function of  $\beta_2$ .

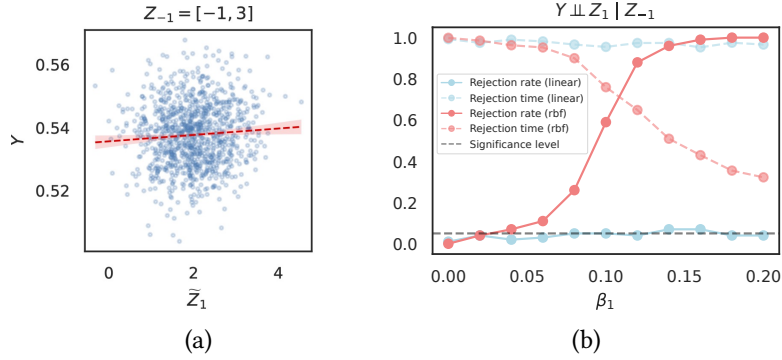


Figure 4: Global conditional importance results for  $H_0 : Y \perp Z_1 \mid Z_{-1}$  with c-SKIT. (a)  $\tilde{Z}_1 \sim P_{Z_1|Z_{-1}}$  is independent of  $Y$  for  $Z_{-1} = [-1, 3]$ . As expected, the slope of the linear regression between  $Y$  and  $\tilde{Z}_1$  is  $\approx 0$ . (b) Mean rejection rate and mean rejection time for c-SKIT with a linear and RBF kernel, as a function of  $\beta_1$ .

analytically as shown in Eq. (24). We verify the conditional distribution behaves as expected in Fig. 4a. By construction,  $\tilde{Z}_1$  is sampled without looking at  $Y$ , hence it is independent, and, as expected, the slope of the linear regression (red dashed line) is  $\approx 0$ . Fig. 4b shows mean rejection rate and time as a function of  $\beta_1$ . First and foremost, we can see that in this case the linear kernel always fails to reject—independently of the value of  $\beta_1$ . This behavior highlights an important aspect of all kernel-based tests, that is the kernel needs to be *characteristic* for the mean embedding to be an injective function [24, 65]. If this condition is not satisfied, different probability distributions may have the same mean embedding in the RKHS, and it may not be possible to disambiguate them at all. Consequently, the test will not be consistent, and increasing  $\tau^{\max}$  will not increase power. For the RBF kernel—which satisfies the characteristic property for probability distributions on  $\mathbb{R}^d$ —the test is valid (i.e., it provides Type I error control for  $\beta_1 = 0$ ), and it is adaptive to the strength of the conditional dependence structure—as  $\beta_1$  increases, the rejection time decreases.

#### 4.1.3 Local Conditional Importance with x-SKIT

Finally, we test that for a fixed  $z$ ,

$$z_3 = 0 \implies g(\tilde{Z}_{\{2,3\}}) \stackrel{d}{=} g(\tilde{Z}_3), \quad \tilde{Z}_C \sim P_{Z|Z_C=z_C}, \quad \forall C \subseteq [m]. \quad (27)$$

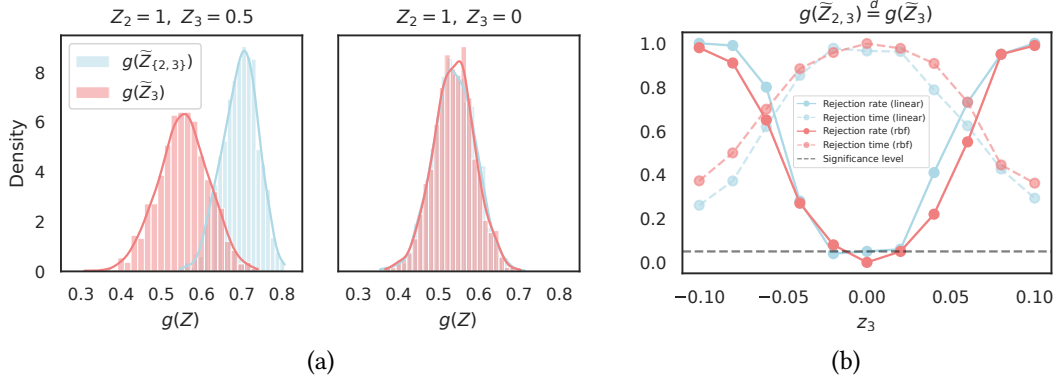


Figure 5: Local conditional importance results for  $H_0 : g(\tilde{Z}_{\{2,3\}}) \stackrel{d}{=} g(\tilde{Z}_3)$  with x-SKIT. (a) Shows that, as expected, the test and null distributions overlap when  $z_3 = 0$ .

with x-SKIT (Algorithm 3). That is—because of the multiplicative term  $z_2 z_3$  in  $g$ —the observed value of  $z_2$  does not change the distribution of the response of the model when  $z_3 = 0$ . Fig. 5a shows the test (i.e.,  $g(\tilde{Z}_{\{2,3\}})$ ) and null (i.e.,  $g(\tilde{Z}_3)$ ) distributions for different values of  $z_3$  when  $z_2 = 1$ . As expected, we can see that when  $z_3 = 0$ , the two distributions overlap, whereas when  $z_3 = 0.5$ , the test distribution is slightly shifted to the right. Fig. 5b shows results of x-SKIT with both a linear and RBF kernel as a function of  $z_3$ . We use both positive and negative values of  $z_3$  to show that x-SKIT has a two-sided alternative, i.e. it rejects both when the test distribution is to the right and to the left of the null. We can see that both the linear and RBF kernel provide Type I error control for when  $z_3 = 0$ , and that their rejection times adapt to the hardness of the problem.

Now that we have illustrated all tests in arguably the simplest setting, we move onto a synthetic dataset where the response is learned by means of a neural network.

## 4.2 Counting MNIST Digits

In this section, we test the semantic importance structure of a neural network trained to count numbers in synthetic images assembled by placing digits from the MNIST dataset [37] in a  $4 \times 4$  grid. Fig. 6 depicts the data-generating process, which satisfies:

- Blue zeros, orange threes, blue twos, and purple sevens are sampled independently with

$$Z_{\text{blue zeros}} \sim \mathcal{U}(\{0, 1, 2\}) + \epsilon \quad Z_{\text{orange threes}} \sim \mathcal{U}(\{0, 1, 2\}) + \epsilon \quad (28)$$

$$Z_{\text{blue twos}} \sim \mathcal{U}(\{1, 2\}) + \epsilon \quad Z_{\text{purple sevens}} \sim \mathcal{U}(\{1, 2\}) + \epsilon \quad (29)$$

- Green fives are sampled conditionally on blue zeros with

$$Z_{\text{green fives}} \mid Z_{\text{blue zeros}} \sim \text{Cat} \left( \{1, 2, 3\}, \begin{cases} [3/4, 1/8, 1/8] & \text{if } N_{\text{blue zeros}} = 0 \\ [1/8, 3/4, 1/8] & \text{if } N_{\text{blue zeros}} = 1 \\ [1/8, 1/8, 3/4] & \text{if } N_{\text{blue zeros}} = 2 \end{cases} \right) + \epsilon. \quad (30)$$

That is, the number of blue zeros changes the probability distribution of green fives over 1,2,3.



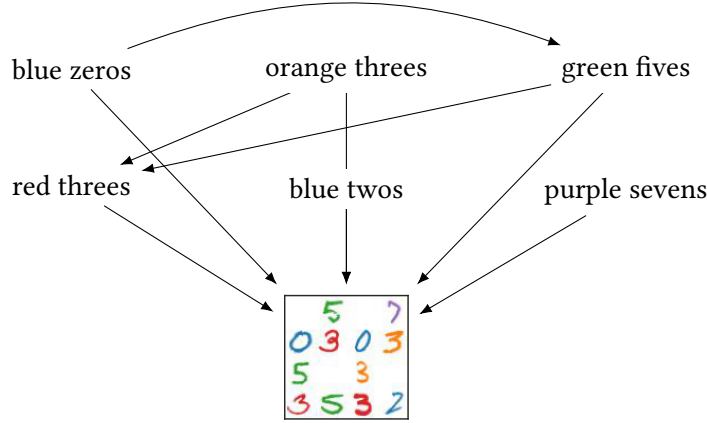


Figure 6: Pictorial representation of the data-generating process for the counting dataset.

- Red threes are sampled conditionally on both orange threes and green fives with

$$Z_{\text{red threes}} \mid Z_{\text{orange threes}}, Z_{\text{green fives}} \sim 2 + \text{Bernoulli}(p) + \epsilon, \quad (31)$$

$$p = \begin{cases} \alpha & \text{if } N_{\text{orange threes}} N_{\text{green fives}} \geq 3 \\ 1 - \alpha & \text{otherwise} \end{cases}, \quad \alpha = 0.9. \quad (32)$$

That is, the product of the number of orange threes and green fives changes the distribution of red threes over 1,2.

Finally, we remark that  $N$  denotes the nearest integer to  $Z$ , and  $\epsilon$  is independent uniform noise (i.e.,  $\epsilon \sim \mathcal{U}((-0.5, 0.5))$ ) to make the distribution of the concepts continuous. To summarize, in order to generate images, we first sample the concepts  $Z$  according to the distribution above, round their values to their respective nearest integers  $N$ , and finally randomly place digits from the MNIST dataset in a  $4 \times 4$  grid according to their number. Note that this data-generating process adds color to the original black and white MNIST digits, and that color matters for the counting task since there are both orange and red threes.

We remark that, with the data generating process above, we can sample from the true conditional distribution of the digits, and, consequently, of images. We omit details on the conditional distribution for the sake of presentation (all code necessary to reproduce experiments will be included). We stress that this differs slightly from the general setting presented in this paper, where we consider both an encoder  $f$  and a classifier  $g$  such that  $\hat{y} = g(f(x))$ , and we sample from the conditional distribution of the dense embeddings  $H$  given any subset of concepts (i.e.,  $P_{H|Z_C}$ ). The scope of this experiment is to showcase the effectiveness of our tests when the response is parametrized by a complex, nonlinear, learned predictor, hence we train a neural network such that  $\hat{y} = f(x)$  and directly sample from the conditional distribution of images given any subset of digits (i.e.,  $P_{X|Z_C}$ ).

We sample a training dataset of 50,000 images and train a ResNet18 [29] to predict the number of all digits for 6 epochs with batch size of 64 and Adam optimizer [34] with learning rate equal to  $10^{-4}$ , weight decay of  $10^{-5}$ , and a scheduler that halves the learning rate every other epoch (recall that the model needs to learn to disambiguate red and orange threes, so color matters). To evaluate the model, we round predictions to the nearest integer and compute accuracy on a held-out set of 10,000 images from the same distribution (we use the original train and test splits of the MNIST dataset to guarantee no digits showed during training are included in test images), and the model achieves an accuracy greater than 99%.

Herein, we study the semantic importance structure of the *predicted* number of red threes with respect to the *predicted* number of other digits. Note that the ground-truth distribution satisfies the following

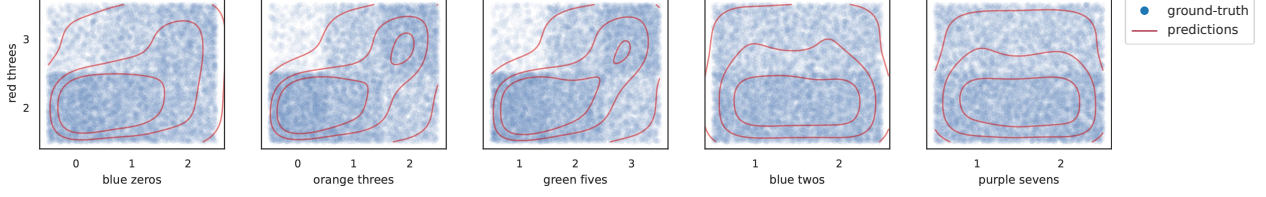


Figure 7: Distribution of ground-truth data and density estimation of the predictions of the trained model for the validation data in the counting digits experiments.

conditions:

1. Red threes are independent of blue twos and purple sevens, i.e.

$$Z_{\text{red threes}} \perp\!\!\!\perp Z_{\text{blue twos}} \quad \text{and} \quad Z_{\text{red threes}} \perp\!\!\!\perp Z_{\text{purple sevens}}. \quad (33)$$

2. Red threes are independent of blue zeros conditionally on green fives, i.e.

$$Z_{\text{red threes}} \perp\!\!\!\perp Z_{\text{blue zeros}} \mid Z_{\text{green fives}}. \quad (34)$$

3. If—in a specific image—there are no orange threes, then red threes are independent of green fives, i.e.

$$Z_{\text{red threes}} \mid (N_{\text{green fives}} = n_{\text{green fives}}, N_{\text{orange threes}} = 0) \stackrel{d}{=} Z_{\text{red threes}} \mid N_{\text{orange threes}} = 0. \quad (35)$$

#### 4.2.1 Global Importance with SKIT

We start by testing whether the predictions of the model satisfy the ground-truth condition

$$Z_{\text{red threes}} \perp\!\!\!\perp Z_{\text{blue twos}} \quad \text{and} \quad Z_{\text{red threes}} \perp\!\!\!\perp Z_{\text{purple sevens}} \quad (36)$$

with SKIT (Algorithm 1). We remark that at inference, we round predictions to the nearest integer and add independent uniform noise  $\epsilon \sim \mathcal{U}((-0.5, 0.5))$  to make the distribution of the response of the model continuous. Fig. 7 shows the ground-truth distribution of red threes as a function of other digits in the held-out set, and the kernel density estimation of the predictions of the model. As expected, we can see that the ground-truth distribution is marginally dependent on blue zeros, orange threes, and green fives, but it is independent of blue twos and purple sevens.

We repeat all tests 100 times with both linear and RBF kernels with bandwidth set to the median of the pairwise distances of previous observations. We perform tests on independent draws of data of size  $\tau^{\max} \in \{100, 200, 400, 800, 1600\}$  from the validation set, and study the rank of importance as a function of  $\tau^{\max}$ , i.e. the amount of data available to test. Fig. 8 includes mean rejection rate and mean rejection time for each digit, and the rank of importance of digits as a function of  $\tau^{\max}$ . We can see that—as expected—both linear and RBF kernels successfully control Type I error for “blue twos” and “purple sevens”, and this confirms that the distribution of the predictions of the model agrees with the underlying ground-truth data-generating process. Furthermore, we can see that the rank of importance is stable across different values of  $\tau^{\max}$ , with purple sevens and blue twos consistently ranked last.

#### 4.2.2 Global Conditional Importance with c-SKIT

Then, we test whether the predictions of the model satisfy the ground-truth conditional independence condition

$$Z_{\text{red threes}} \perp\!\!\!\perp Z_{\text{blue zeros}} \mid Z_{\text{green fives}} \quad (37)$$

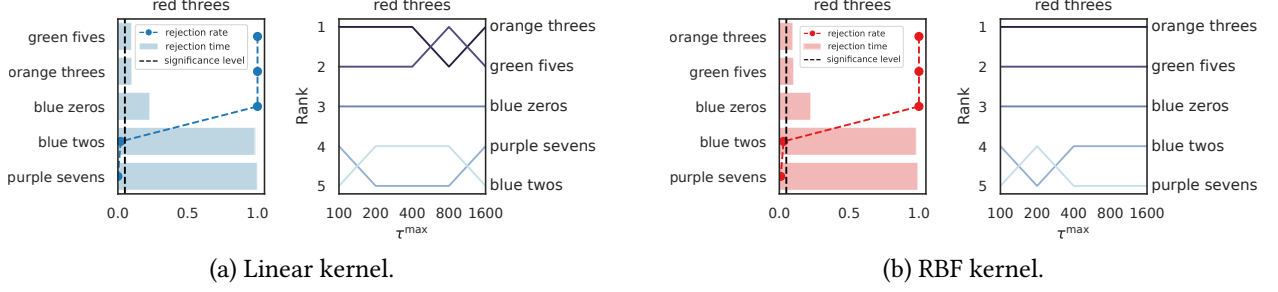


Figure 8: Global semantic importance results for the predicted number of red threes with linear and RBF kernels. In each subfigure, the leftmost panel shows mean rejection rate and mean rejection time over 100 tests with  $\alpha = 0.05$  and  $\tau^{\max} = 800$ . The rightmost panel shows the rank of importance of digits for the prediction of red threes as a function of  $\tau^{\max}$ .

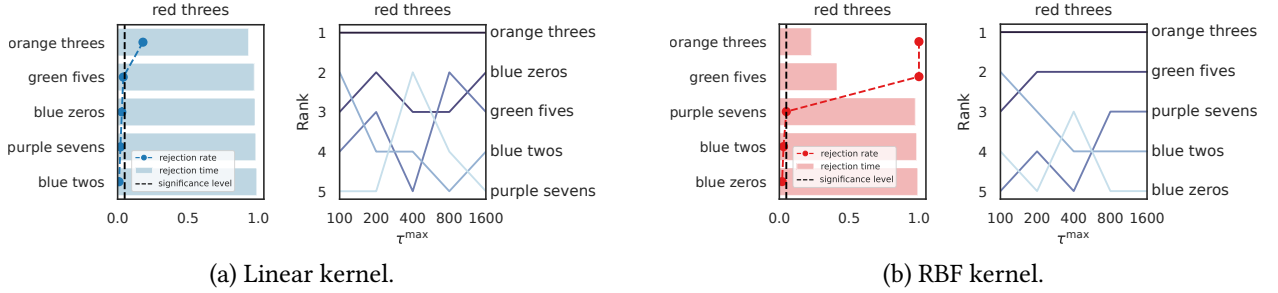


Figure 9: Global conditional semantic importance results for the predicted number of red threes with linear and RBF kernels. In each subfigure, the leftmost panel shows mean rejection rate and mean rejection time over 100 tests with  $\alpha = 0.05$  and  $\tau^{\max} = 800$ . The rightmost panel shows the rank of importance of digits for the prediction of red threes as a function of  $\tau^{\max}$ .

with c-SKIT. Analogous to above, we repeat all tests 100 times with linear and RBF kernels, and Fig. 9 include results for  $\tau^{\max} \in \{100, 200, 400, 800, 1600\}$ . Here—similarly to the synthetic experiment presented in Section 4.1—we can see that the linear kernel almost always fails to reject, i.e. the mean rejection rates for all digits are close to 0. As discussed earlier, this behavior is due to the fact that the linear kernel is not characteristic for the distributions. On the other hand, the RBF is, and, as expected, it is consistent and it provides Type I error control for the null hypothesis that red threes are independent of blue zeros conditionally on all other digits, which is true. Furthermore, we can see that the rank of importance is less stable compared to the one in Fig. 3, and in particular,  $\tau^{\max} = 100$  seems not to be sufficient to retrieve the correct ground-truth structure (i.e., blue twos are ranked before green fives). This highlights how the amount of data available for testing may affect results and findings.

#### 4.2.3 Local Conditional Importance with x-SKIT

Finally, we test whether the predictions of the model satisfy the ground-truth condition that, for a particular image, if there are no orange threes (i.e.,  $n_{\text{orange threes}} = 0$ ) then red threes are independent of the observed green fives (i.e.,  $n_{\text{green fives}}$ ), i.e.

$$Z_{\text{red threes}} | (N_{\text{green fives}} = n_{\text{green fives}}, N_{\text{orange threes}} = 0) \stackrel{d}{=} Z_{\text{red threes}} | N_{\text{orange threes}} = 0. \quad (38)$$

We remark that, in the equation above, conditioning is written in terms of the integer  $n_{\text{orange threes}} = 0$  because of its intuitive meaning, and that this is equivalent to conditioning on  $z_{\text{orange threes}} \in (-0.5, 0.5)$ .

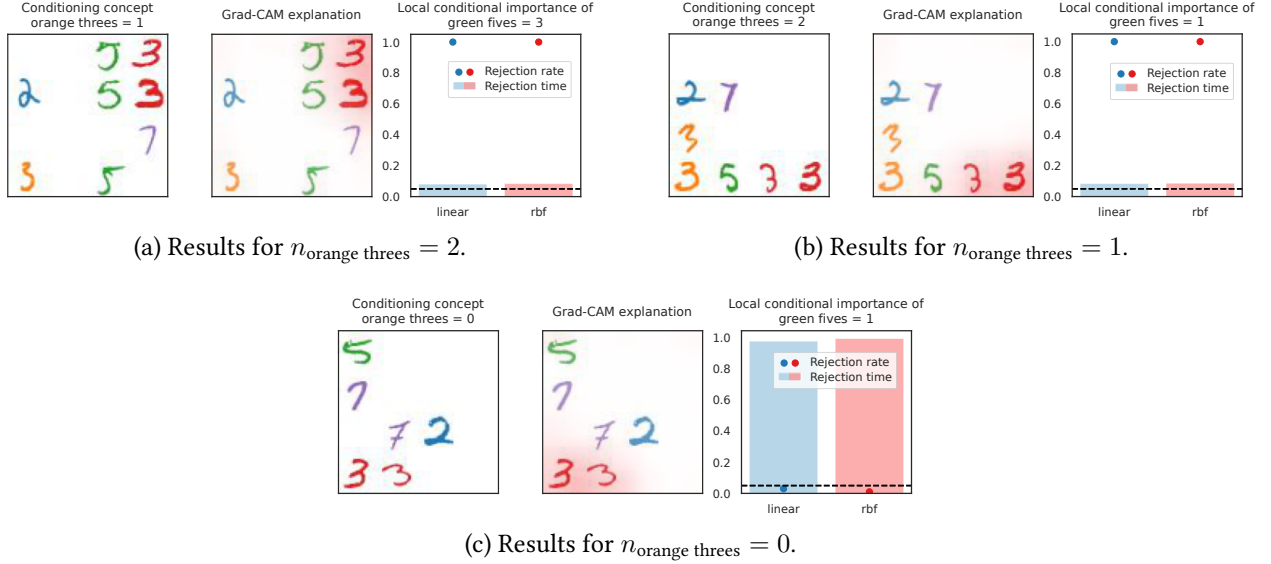


Figure 10: Local conditional importance of  $N_{\text{green fives}}$  conditionally on  $N_{\text{orange threes}}$ . Each row contains the input image, the Grad-CAM explanation for the prediction of the model, and x-SKIT results for 100 repetitions of the test with  $\tau^{\max} = 400$ , with a linear and RBF kernel. Note that x-SKIT finds the observed number of green fives important whenever the number of orange threes is greater than zero, whereas Grad-CAM does not.

Similarly, we could replace  $n_{\text{green fives}}$  with  $z_{\text{green fives}}$ , and, in practice, we run tests conditioning on the observed concepts  $z$ , and not their integer values  $n$ .

We use x-SKIT (Algorithm 3) with a linear and RBF kernel with bandwidth set to the median of the pairwise distances of previous observations. We repeat all tests 100 times on individual images with 0, 1, and 2 orange threes, significance level  $\alpha = 0.05$ , and  $\tau^{\max} = 400$ . Fig. 10 shows results grouped by number of orange threes. As expected, we see that when  $n_{\text{orange threes}}$  is greater than 0, the number of green fives is important for the predictions of the model (i.e., rejection rate is close to 1, with short rejection rate), whereas when there are no orange threes in the image, both the linear and RBF kernel control Type I error. We qualitatively compared our findings with pixel-level explanations with Grad-CAM [55], and we can see that they only highlight red threes because that is the digit we are explaining the prediction of. That is, pixel-level explanations cannot convey the full spectrum of semantic importance for the predictions of a model—which can be misleading to users. For example, in this case, a user may not understand when the predictions of a model depend on the number of green fives, because they are never highlighted by pixel-level saliency maps. In real-world scenarios, digits may be replaced by sensitive attributes that cannot be inferred by the raw value of pixels. For example, a saliency map highlighting a face does not convey which attributes were used by the model, such as skin color, biological sex, or gender. It is immediate to see how being able to investigate the dependencies of the predictions of a model with respects to these attributes (which our definitions provide) is paramount for their safe deployment.

With these results on synthetic datasets, we now showcase the flexibility of our proposed tests on zero-shot image classification with CLIP [49].

## 5 Real-world Experiments

In this section, we showcase the flexibility and effectiveness of our framework on zero-shot image classification on three real-world datasets: animals with attributes 2 (AwA2) [79], CUB-200-2011 (CUB) [74],

Table 1: Comparison of SKIT, c-SKIT, and PCBM on the AwA2 dataset.

Importance	Accuracy	Rank agreement	Importance $f_1$ score
<b>SKIT</b>	<b>99.50% <math>\pm</math> 0.88%</b>	<b>0.50 <math>\pm</math> 0.20</b>	<b>0.65 <math>\pm</math> 0.11</b>
<b>c-SKIT</b>	<b>99.50% <math>\pm</math> 0.88%</b>	0.46 $\pm$ 0.17	0.57 $\pm$ 0.11
PCBM	95.11% $\pm$ 4.82%	0.36 $\pm$ 0.22	0.53 $\pm$ 0.14

and the Imagenette subset of ImageNet [21] (available at <https://github.com/fastai/imagenette>). We compare performance and transferability of the ranks of importance across 8 different vision-language models, both CLIP- and non-CLIP-based. For all experiments,  $f$  is the image encoder of the vision-language model, and  $g$  is the (linear) zero-shot classifier constructed by encoding “A photo of a <CLASS\_NAME>” with the text encoder.

Recall that, in order to run our c-SKIT and x-SKIT tests, we need to sample from  $P_{Z_j|Z_{-j}}$  and  $P_{H|Z_C=z_C}$ ,  $C \subseteq [m]$ , respectively. These distributions are generally not known, and here—since  $m$  is small—we propose to use nonparametric methods to estimate them from data. We refer interested readers to Appendix D.1 for details. Herein, we will always use RBF kernels to estimate the appropriate MMD in each test, and we will set their scales to specific quantiles of the pairwise distances of the observations. We repeat each test 100 times on independent draws of  $\tau^{\max}$  samples, and estimate each concept’s *expected rejection time* and *expected rejection rate* at a significance level of  $\alpha = 0.05$  with the FDR post-processor described in Algorithm 4. That is, a (normalized) rejection time equal to 1 means failing to reject in  $\tau^{\max}$  steps. We briefly list the models we use and the way we evaluate agreement among them.

**List of vision-language models:** CLIP:RN50,ViT-B/32,ViT-L/14 [49], OpenClip:ViT-B-32,ViT-L-14 [30], FLAVA [63], ALIGN [31], and BLIP [38].

**Evaluating rank agreement:** We use a weighted version of Kendall’s tau [32] introduced by Vigna [71], which assigns higher penalties to swaps between elements with higher ranks. This choice reflects the fact that concepts with higher importance should be more stable across different models. We briefly remark that this notion of rank agreement is bounded in  $[-1, 1]$  ( $-1$  indicates reverse order, and  $1$  perfect alignment) but not symmetric.

**Evaluating importance agreement:** We threshold rejection rates at level  $\alpha$  to classify concepts into important and not important ones. Then, importance agreement is the accuracy between pairs of binarized vectors.

We now present results on each dataset.

## 5.1 AwA2 Dataset

The AwA2 dataset comprises 37,322 images (29,841 for training and 7,481 for testing) from 50 animal species with class-level annotations of 85 attributes. Concept annotations are reported both as frequencies (i.e., how often an attribute appears in images coming from a class) and as binary labels (i.e., 1 means that an attribute is present in a class, and 0 otherwise). Given the presence of global (i.e., class-level) labels, we use SKIT and c-SKIT to test the global (and global conditional) semantic importance structure of the predictions for the top-10 best classified animal categories across models. For each class, we test 20 attributes ( $m = 20$ ): the 10 most frequent, and a random subset of 10 absent ones (see Fig. D.3 for some example images and Table D.2 for the concepts used in this experiment), and, for each model, we obtain the dictionary  $c$  with its text encoder. Tests are run with bandwidths of the kernels set to the 90<sup>th</sup> percentile of the pairwise distances and  $\tau^{\max} = 400, 800$  for SKIT and c-SKIT, respectively.

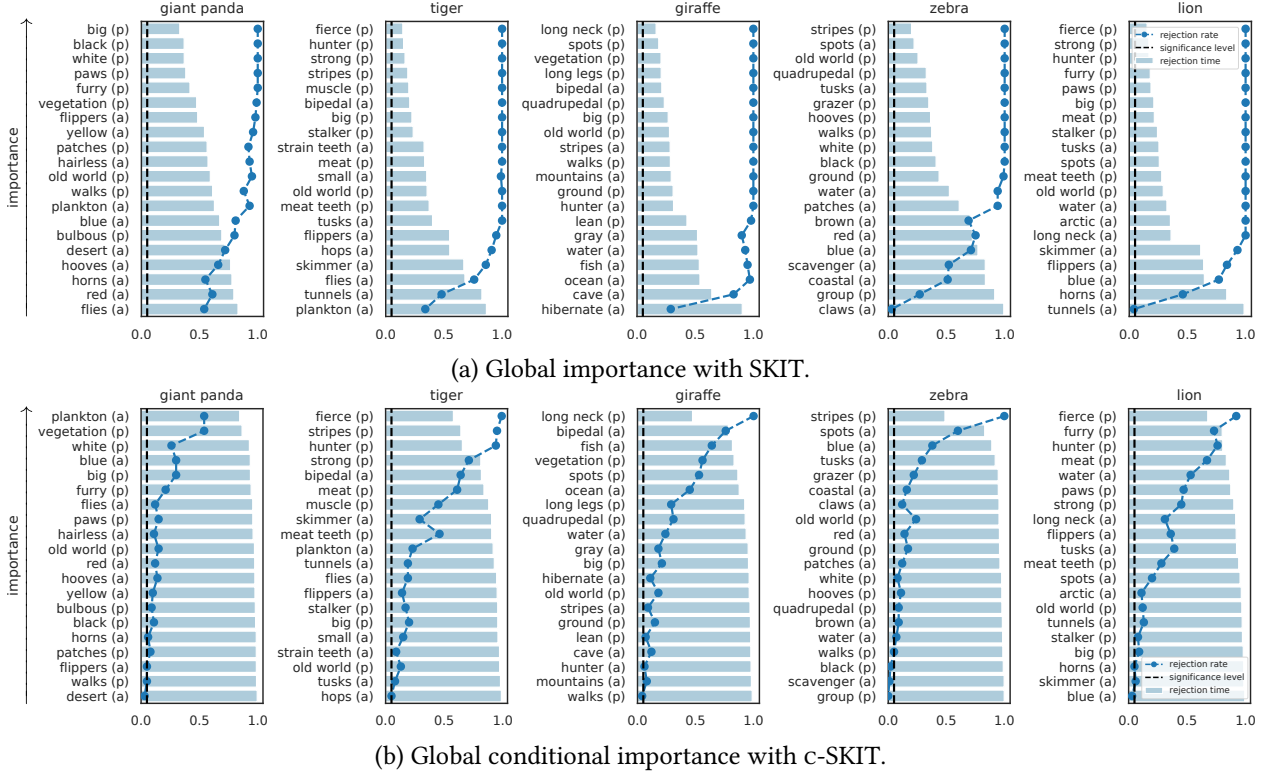


Figure 11: Example ranks of global marginal and global conditional importance on CLIP:ViT-L/14 for the first 5 test classes in the AwA2 dataset. Concepts are annotated with  $(p)$  if they are present in the class according to the ground-truth annotations, and with  $(a)$  otherwise.

Table 1 compares SKIT, c-SKIT, and PCBM in terms of classification accuracy, rank agreement, and importance detection  $f_1$  score. Intuitively, we would expect concepts that are absent from a particular animal species not to be relevant for the predictions of a model. So, we classify the top-10 concepts reported by each method as important, and we compute the  $f_1$  score with the ground-truth annotations. When comparing with PCBM—since we use different concepts for each class—we train 100 independent linear models for each class and rank concepts based on their average absolute weights. We use absolute weights and not signed ones because the null hypotheses presented in this work are two-sided, i.e. a concept is important both if it increases the prediction for a class or if it decreases it. SKIT and c-SKIT outperform PCBM across all three metrics (SKIT and c-SKIT have the same accuracy because they do not change the original predictor), with SKIT providing the highest rank agreement and importance  $f_1$  score. Interestingly, ranks provided by our tests are more transferable across models, which suggests the latter may share a similar semantic (conditional) independence structure notwithstanding their embedding size or training strategy. We refer interested readers to Fig. D.4 for all individual pairwise agreements between models.

Finally, Fig. 11 shows example ranks of global (and global conditional) importance obtained with SKIT and c-SKIT on CLIP:ViT-L/14 for the first 5 test classes (see Figs. D.5 and D.6 for all test classes). We can see that—in general—concepts are globally important (rejection rates are above the significance level  $\alpha$ ), and that it is harder to reject the global conditional null hypothesis (rejection rates are lower and rejection times larger). This reflects the fact that conditional independence is a stronger condition than marginal independence. Finally, we stress that without sequential tests, it would not be possible to break ties among concepts by rejection rates only and provide a rank of importance—which is a fundamental property of our approach.



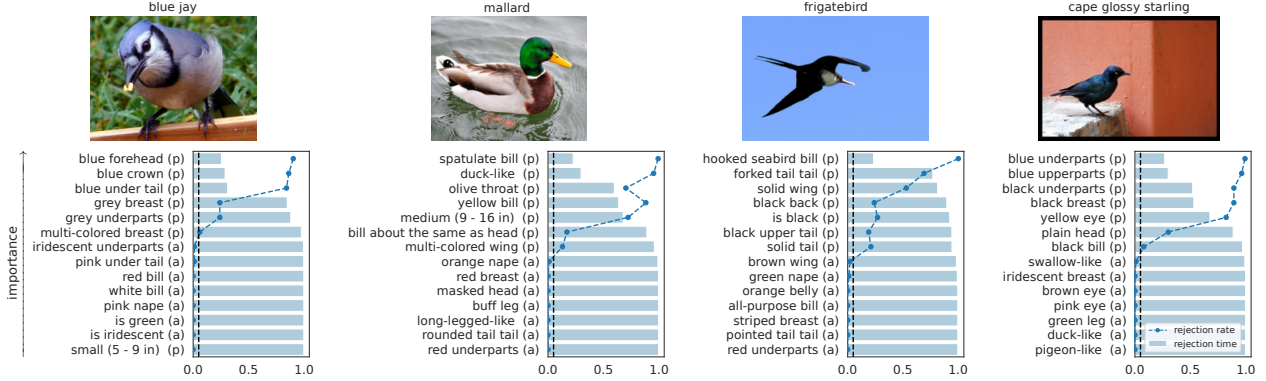


Figure 12: Example ranks of local conditional importance with x-SKIT ( $s = 1$ ) on CLIP:ViT-L/14 for 4 images from the CUB dataset. Concepts are annotated with (p) if they are present in the image according to the ground-truth annotations, and with (a) otherwise.

Table 2: x-SKIT results on the CUB dataset as a function of conditioning set size  $s$ .

$s$	Rank agreement	Importance agreement	Importance $f_1$ score
1	$0.81 \pm 0.14$	$0.96\% \pm 0.06\%$	$0.93 \pm 0.15$
2	$0.82 \pm 0.13$	<b><math>0.97\% \pm 0.06\%</math></b>	<b><math>0.93 \pm 0.14</math></b>
4	<b><math>0.84 \pm 0.12</math></b>	$0.95\% \pm 0.08\%$	$0.88 \pm 0.15$

## 5.2 CUB Dataset

The CUB-200-2011 dataset [74] contains 11,788 images of 200 different bird classes, and each image is annotated with the presence of 312 fine-grained concepts that describe the appearance of the bird (e.g., “has orange bill”, “has hook-shaped bill”, “is small”) with the labelers’ confidence. More formally, the dataset is a collection  $\{(x^{(i)}, y^{(i)}, z^{(i)}, u^{(i)})\}_{i=1}^n$  of images  $x$  with class label  $y$ , binary semantic vector  $z^{(i)} \in \{0, 1\}^m$ , and uncertainty values  $u^{(i)} \in \{1, 2, 3, 4\}^m$ : “not visible” (1), “guessing” (2), “probably” (3), and “definitely” (4). In this experiment, we use x-SKIT to test the conditional semantic importance structure of the predictions of different vision-language models locally on particular images, and we evaluate performance against the ground-truth annotations. We note that the purpose of this experiment is to evaluate the performance of x-SKIT, hence we use the ground-truth semantic annotations as an oracle (instead of predicting the presence of concepts with the models’ text encoders, as we will do in the following experiment). In practical scenarios, however, ground-truth will not be available and one could, as done by previous work [11], use large language models (LLMs) to answer binary queries (e.g., “Does this bird have an orange bill? Yes/No”). Finally, we stress that the attributes annotated in the CUB dataset are fine-grained and require domain expertise that general-purpose vision-language models may not have yet acquired.

Similarly to above, we randomly sample 10 images from the 10 classes with highest average accuracy across models and, for each image, we test 14 concepts. In particular, we first restrict ourselves to annotations with good confidence (i.e., “probably” or “definitely”), and then, for each concept  $j$ , we estimate its marginal (i.e.,  $p_j := \mathbb{P}[Z_j = 1]$ ) and class-conditional (i.e.,  $p_{j|y} := \mathbb{P}[Z_j = 1 | Y = y]$ ) rates over the dataset. Finally, for each test image  $x$  with label  $y$ , we score concepts by the difference between their class-conditional and marginal rates, i.e.  $s_j(y) := p_{j|y} - p_j$ . Intuitively, a large  $s_j(y)$  indicates that concept  $j$  has higher occurrence in class  $y$  compared to the population, and we say that it is *discriminative* for class  $y$ . We test the 7 most discriminative concepts that are present in the observed image  $x$ , and a random subset of 7 concepts that are absent according to the ground-truth annotations. Table D.4 includes the zero-shot accuracy of all models and Fig. D.7 shows example images used in this experiment. We remark that, since concepts are binary, we do not use KDE-based methods as presented in Appendix D.1, and instead we

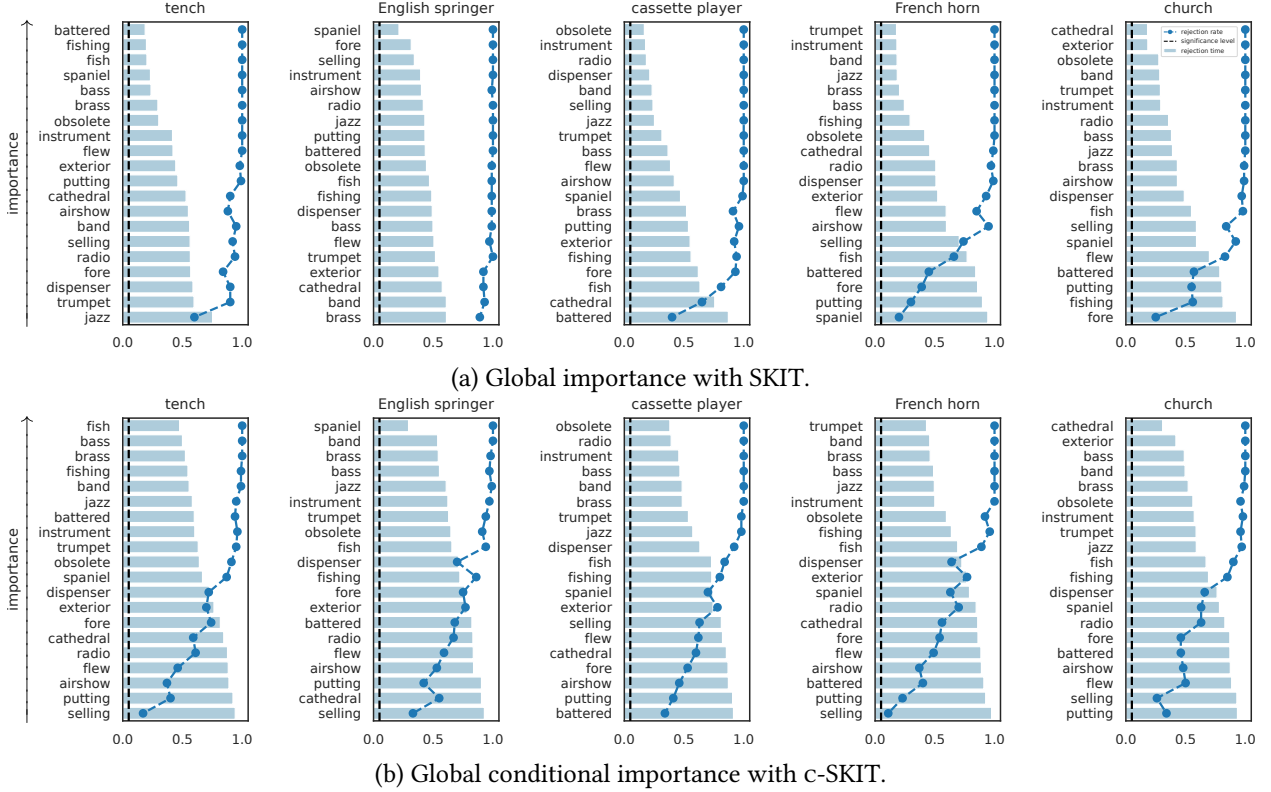


Figure 13: Example ranks of global marginal and global conditional importance on CLIP:ViT-L/14 for the first 5 classes in the Imagenette dataset.

approximate  $P_{H|Z_C=z_C}$  by sampling uniformly from the entries in the dataset that match the conditioning vector  $z_C$ . We use RBF kernels with bandwidths set to the median of the pairwise distances of observations and  $\tau^{\max} = 200$ . Finally, note that for each concept  $j \in [m]$ , there are exponentially many tests with null hypothesis  $H_{0,j,S}^{\text{LC}}$ —one for each subset  $S \subseteq [m] \setminus \{j\}$ —which are intractable to compute. So, we average results over 100 tests with random subsets with fixed size  $s$ . Fig. 12 includes example ranks of importance on CLIP:ViT-L/14 with  $s = 1$  for four images in the CUB dataset (see Fig. D.9 for ranks across all models on the same images).

Table 2 shows average rank and importance agreement alongside importance  $f_1$  score across all models as a function of conditioning set size,  $s$ . We remark that, in this experiment, we classify concepts as important by thresholding their rejection rates at level  $\alpha$ —which is a statistically-valid way of selecting important concepts. Fig. D.8 and Table D.5 include all results for each model individually. These results confirm that ranks of importance are well-aligned both across models and with the ground-truth annotations. We note that the  $f_1$  score for  $s = 4$  (i.e., when conditioning of 4 concepts) is lower compared to  $s = 1, 2$ . This is expected, as the more concepts one conditions on, the smaller the effect of including one additional concept.

### 5.3 Imagenette Dataset

Finally, we use the Imagenette subset of 13,394 images (9,469 for training and 3,925 for testing) from ten easily separable classes in ImageNet [21]. Fig. D.10 includes example images from the classes in the dataset, and Table D.6 reports the classification accuracy across all vision-language models ( $98.99\% \pm 0.01\%$  average accuracy). We note that—differently from the two previous experiments—Imagenette does not provide

Table 3: x-SKIT results on the Imagenette dataset as a function of conditioning set size  $s$ .

$s$	Rank agreement	Importance agreement
1	<b><math>0.59 \pm 0.21</math></b>	<b><math>0.71 \pm 0.14</math></b>
2	$0.56 \pm 0.21$	$0.67 \pm 0.13$
4	$0.53 \pm 0.23$	$0.68 \pm 0.14$

ground-truth semantic annotations to evaluate performance with.

We first test the global (and global conditional) importance of semantic concepts with SKIT and c-SKIT. Since there are no ground-truth semantic annotations, we use SpLiCe [6] to encode the training split of the dataset and keep the top-20 words (i.e.,  $m = 20$ ) as the concepts to test, but we remark that any user-defined set of concepts would be valid. Following previous work [82], we filter the selected concepts such that they are different from the classes in the dataset. In particular, we use the 10,000 most frequent words in the vocabulary from the MSCOCO dataset [39], and we set the  $\ell_1$  regularization term in SpLiCe to 0.20. Furthermore—after running SpLiCe—we use WordNet [22] to lemmatize both concepts and class names (e.g., “churches” becomes “church”) and check that concepts are not contained in class names, and vice versa. For example, the concept “churches” would be skipped because “church” is already the name of a class, and “gasoline” would be skipped because it contains part of the class “gas pump”. For each model, we use its text encoder to obtain the concepts’ embedding.

Fig. 13 shows results for the first 5 classes in the Imagenette dataset using RBF kernels with a bandwidth equal to the 90<sup>th</sup> percentile of the pairwise distances, and  $\tau^{\max} = 400, 800$  for SKIT and c-SKIT, respectively (we refer interested readers to Figs. D.11 and D.12 for ranks of all classes). Analogously to the experiment on the Awa2 dataset, we can see that rejection rates are lower for tests of conditional independence (i.e., c-SKIT) compared to marginal (i.e., SKIT). We evaluate rank agreement across all models and compare with PCBM (which achieves a validation accuracy of  $95.85\% \pm 0.21\%$  across 100 independent duplicates). We found an average rank agreement of  $0.51 \pm 0.21$  for SKIT,  $0.54 \pm 0.19$  for c-SKIT, and  $0.45 \pm 0.21$  for PCBM (see Fig. D.13 for all pairwise values). These results confirm that not only are the ranks produced by our tests more transferable across models, but also they retain the performance of the original classifier. Finally, we qualitatively study the stability of SKIT and c-SKIT ranks as a function of  $\tau^{\max}$ . This is important because  $\tau^{\max}$  is the number of samples available for testing, and it represents the sample complexity of our tests (see Figs. D.14 and D.15 for results). Results suggest that high rank positions (i.e., more important concepts) are more stable than low rank ones (i.e., less important concepts) across different values of  $\tau^{\max}$ , and that SKIT ranks are more stable than c-SKIT ones with smaller values of  $\tau^{\max}$ .

Lastly, we use x-SKIT to test the local conditional semantic importance of the prediction of the models on 2 images for each class in the Imagenette dataset. Here, we use SpLiCe to encode each image and obtain its top-10 words, and then add the bottom-4 concepts according to PCBM, for a total of 14 concepts per image. Recall that we use nonparametric samplers to approximate  $P_{H|Z_C=z_c}$  (see Appendix D.1), so the cost of using image-specific concepts boils down to projecting the feature embeddings with a different matrix  $c$ , which is negligible compared to running the tests. We note that parametric generative models—such as variational autoencoders or diffusion models—would have required retraining for each set of concepts, which is expensive. Table 3 summarizes rank and importance agreement as a function of conditioning set size for RBF kernels with bandwidths set to the median of the pairwise distances, and  $\tau^{\max} = 200$  (see Fig. D.16 for all pairwise comparisons). Overall, ranks are well-aligned across models, with  $s = 1$  as the optimal conditioning set size (rank agreement  $0.59 \pm 0.21$  and importance agreement  $0.71 \pm 0.14$ ). First, we note that ranks of local conditional importance with x-SKIT are slightly better-aligned compared to global (and global conditional) importance with SKIT and c-SKIT. Furthermore, both rank and importance agreements are lower compared to the CUB dataset. This is because (i) in the CUB dataset, we use the ground-truth binary annotations as semantics  $z$  instead of predicting them with the models’ text encoders,

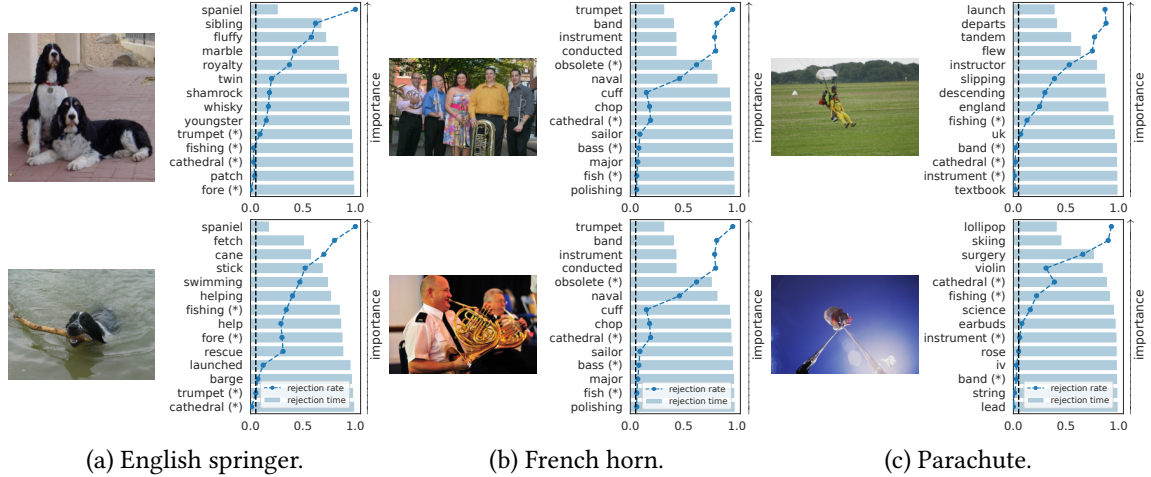


Figure 14: Example ranks of local conditional importance with x-SKIT ( $s = 1$ ) on CLIP:ViT-L/14 for 2 images from 3 classes from the Imagenette dataset. The 4 least important concepts according to PCBM are annotated with (\*).

and (ii) here, we need to approximate the conditional distribution  $P_{H|Z_C=z_C}$ . Furthermore, since we do not have access to ground-truth semantic annotations to evaluate importance detection  $f_1$  score, we plan to design user-studies to quantitatively evaluate the alignment of the produced ranks with human intuition, and we regard this as future work. Importantly, we remark that no other method is currently available to execute such user-studies.

Fig. 14 shows example results on CLIP:ViT-L/14 for 2 images from 3 classes in the Imagenette dataset (see Fig. D.17 for ranks on the same images across all models). We can appreciate how the bottom-4 concepts from PCBM, which are annotated with an asterisk (\*), are not always last, i.e. a concept may be locally important even if it is not globally important. For example, concept “fishing” may not be globally important for class “English springer”, but it is locally important for an image of a dog in water. Conversely, a concept having a high weight according to SpLiCe does not imply it will be statistically important for the predictions of the model, and these distinctions are important in order to communicate findings transparently to users.

## 6 Conclusions

There exist an increasing interest in explaining modern, unintelligible predictors and, in particular, doing so with inherently interpretable concepts that convey specific meaning to users. This work is the first to formalize precise statistical notions of semantic importance in terms of global (i.e., over a population) and local (i.e., on a sample) conditional hypothesis testing. Not only do we propose novel, valid tests for each notion of importance, but also provide a rank of importance by deploying ideas of sequential testing. Importantly, by approaching importance via conditional independence (and by developing appropriate valid tests), we are able to provide Type I error and FDR control, a feature that is unique to our framework compared to existing alternatives. Furthermore, our tests allow us to explain the original—potentially nonlinear—classifier that would be used in the wild, as opposed to training surrogate linear models as has been the standard so far.

Naturally, our work has limitations. First and foremost, the procedures introduced in this work require access to samplers, and there might be settings where learning these models is hard; we used nonparametric estimators in our experiments, but modern generative models could be employed, too. Second, kernel-based tests rely on the assumption that the kernels used are characteristic for the space of distributions considered. Although these assumptions are usually satisfied in  $\mathbb{R}^d$  for RBF kernels, there may exist data modalities

where this is not true (e.g., discrete data, graphs), which would compromise the power of the test. Finally, although we grant full flexibility to users to specify the concepts they care about, there is no guarantee that these are well-represented in the feature space of the model, nor that they are the most informative ones for a specific task. All these points are a matter of ongoing and future work.

## Acknowledgments

We thank Zhenzhen Wang for useful conversations that strengthened the presentation of our experimental results. This research was supported by NSF CAREER Award CCF 2239787.

## References

- [1] Nachman Aronszajn. Theory of reproducing kernels. *Transactions of the American mathematical society*, 68(3):337–404, 1950.
- [2] David Bau, Bolei Zhou, Aditya Khosla, Aude Oliva, and Antonio Torralba. Network dissection: Quantifying interpretability of deep visual representations. In *Proceedings of the IEEE conference on computer vision and pattern recognition*, pages 6541–6549, 2017.
- [3] Yoav Benjamini and Yosef Hochberg. Controlling the false discovery rate: a practical and powerful approach to multiple testing. *Journal of the Royal statistical society: series B (Methodological)*, 57(1): 289–300, 1995.
- [4] Alain Berlinet and Christine Thomas-Agnan. *Reproducing kernel Hilbert spaces in probability and statistics*. Springer Science & Business Media, 2011.
- [5] Thomas B Berrett, Yi Wang, Rina Foygel Barber, and Richard J Samworth. The conditional permutation test for independence while controlling for confounders. *Journal of the Royal Statistical Society Series B: Statistical Methodology*, 82(1):175–197, 2020.
- [6] Usha Bhalla, Alex Oesterling, Suraj Srinivas, Flavio P Calmon, and Himabindu Lakkaraju. Interpreting clip with sparse linear concept embeddings (splice). *arXiv preprint arXiv:2402.10376*, 2024.
- [7] Gilles Blanchard and Etienne Roquain. Two simple sufficient conditions for fdr control. *Electronic Journal of Statistics*, 2:963–992, 2008.
- [8] Carlo Bonferroni. Teoria statistica delle classi e calcolo delle probabilita. *Pubblicazioni del R istituto superiore di scienze economiche e commerciali di firenze*, 8:3–62, 1936.
- [9] Collin Burns, Jesse Thomason, and Wesley Tansey. Interpreting black box models via hypothesis testing. In *Proceedings of the 2020 ACM-IMS on foundations of data science conference*, pages 47–57, 2020.
- [10] Emmanuel Candes, Yingying Fan, Lucas Janson, and Jinchi Lv. Panning for gold: ‘model-x’ knockoffs for high dimensional controlled variable selection. *Journal of the Royal Statistical Society Series B: Statistical Methodology*, 80(3):551–577, 2018.
- [11] Aditya Chattopadhyay, Kwan Ho Ryan Chan, and Rene Vidal. Bootstrapping variational information pursuit with large language and vision models for interpretable image classification. In *The Twelfth International Conference on Learning Representations*, 2024.

- [12] Aditya Chattopadhyay, Ryan Pilgrim, and Rene Vidal. Information maximization perspective of orthogonal matching pursuit with applications to explainable ai. *Advances in Neural Information Processing Systems*, 36, 2024.
- [13] Haozhe Chen, Junfeng Yang, Carl Vondrick, and Chengzhi Mao. Invite: Interpret and control vision-language models with text explanations. In *The Twelfth International Conference on Learning Representations*.
- [14] Jianbo Chen, Le Song, Martin J Wainwright, and Michael I Jordan. L-shapley and c-shapley: Efficient model interpretation for structured data. *arXiv preprint arXiv:1808.02610*, 2018.
- [15] Mehdi Cherti, Romain Beaumont, Ross Wightman, Mitchell Wortsman, Gabriel Ilharco, Cade Gordon, Christoph Schuhmann, Ludwig Schmidt, and Jenia Jitsev. Reproducible scaling laws for contrastive language-image learning. In *Proceedings of the IEEE/CVF Conference on Computer Vision and Pattern Recognition*, pages 2818–2829, 2023.
- [16] Thomas M Cover. Universal portfolios. *Mathematical finance*, 1(1):1–29, 1991.
- [17] Ian Covert, Scott M Lundberg, and Su-In Lee. Understanding global feature contributions with additive importance measures. *Advances in Neural Information Processing Systems*, 33:17212–17223, 2020.
- [18] Ashok Cutkosky and Francesco Orabona. Black-box reductions for parameter-free online learning in banach spaces. In *Conference On Learning Theory*, pages 1493–1529. PMLR, 2018.
- [19] Roxana Daneshjou, Mert Yuksekgonul, Zhuo Ran Cai, Roberto Novoa, and James Y Zou. Skincon: A skin disease dataset densely annotated by domain experts for fine-grained debugging and analysis. *Advances in Neural Information Processing Systems*, 35:18157–18167, 2022.
- [20] Marina Danilevsky, Kun Qian, Ranit Aharonov, Yannis Katsis, Ban Kawas, and Prithviraj Sen. A survey of the state of explainable ai for natural language processing. *arXiv preprint arXiv:2010.00711*, 2020.
- [21] Jia Deng, Wei Dong, Richard Socher, Li-Jia Li, Kai Li, and Li Fei-Fei. Imagenet: A large-scale hierarchical image database. In *2009 IEEE conference on computer vision and pattern recognition*, pages 248–255. Ieee, 2009.
- [22] Christiane Fellbaum. *WordNet: An electronic lexical database*. MIT press, 1998.
- [23] Lasse Fischer and Aaditya Ramdas. Sequential permutation testing by betting. *arXiv preprint arXiv:2401.07365*, 2024.
- [24] Kenji Fukumizu, Arthur Gretton, Xiaohai Sun, and Bernhard Schölkopf. Kernel measures of conditional dependence. *Advances in neural information processing systems*, 20, 2007.
- [25] Yossi Gandelsman, Alexei A Efros, and Jacob Steinhardt. Interpreting clip’s image representation via text-based decomposition. *arXiv preprint arXiv:2310.05916*, 2023.
- [26] Damien Garreau, Wittawat Jitkrittum, and Motonobu Kanagawa. Large sample analysis of the median heuristic. *arXiv preprint arXiv:1707.07269*, 2017.
- [27] Arthur Gretton, Kenji Fukumizu, Choon Teo, Le Song, Bernhard Schölkopf, and Alex Smola. A kernel statistical test of independence. *Advances in neural information processing systems*, 20, 2007.
- [28] Arthur Gretton, Karsten M Borgwardt, Malte J Rasch, Bernhard Schölkopf, and Alexander Smola. A kernel two-sample test. *The Journal of Machine Learning Research*, 13(1):723–773, 2012.



- [29] Kaiming He, Xiangyu Zhang, Shaoqing Ren, and Jian Sun. Deep residual learning for image recognition. In *Proceedings of the IEEE conference on computer vision and pattern recognition*, pages 770–778, 2016.
- [30] Gabriel Ilharco, Mitchell Wortsman, Ross Wightman, Cade Gordon, Nicholas Carlini, Rohan Taori, Achal Dave, Vaishaal Shankar, Hongseok Namkoong, John Miller, Hannaneh Hajishirzi, Ali Farhadi, and Ludwig Schmidt. Openclip, July 2021. URL <https://doi.org/10.5281/zenodo.5143773>. If you use this software, please cite it as below.
- [31] Chao Jia, Yinfei Yang, Ye Xia, Yi-Ting Chen, Zarana Parekh, Hieu Pham, Quoc Le, Yun-Hsuan Sung, Zhen Li, and Tom Duerig. Scaling up visual and vision-language representation learning with noisy text supervision. In *International conference on machine learning*, pages 4904–4916. PMLR, 2021.
- [32] Maurice G Kendall. A new measure of rank correlation. *Biometrika*, 30(1-2):81–93, 1938.
- [33] Been Kim, Martin Wattenberg, Justin Gilmer, Carrie Cai, James Wexler, Fernanda Viegas, et al. Interpretability beyond feature attribution: Quantitative testing with concept activation vectors (tcav). In *International conference on machine learning*, pages 2668–2677. PMLR, 2018.
- [34] Diederik P Kingma and Jimmy Ba. Adam: A method for stochastic optimization. *arXiv preprint arXiv:1412.6980*, 2014.
- [35] Pang Wei Koh, Thao Nguyen, Yew Siang Tang, Stephen Mussmann, Emma Pierson, Been Kim, and Percy Liang. Concept bottleneck models. In *International conference on machine learning*, pages 5338–5348. PMLR, 2020.
- [36] Stefan Kolek, Aditya Chattopadhyay, Kwan Ho Ryan Chan, Hector Andrade-Loarca, Gitta Kutyniok, and René Vidal. Learning interpretable queries for explainable image classification with information pursuit. *arXiv preprint arXiv:2312.11548*, 2023.
- [37] Yann LeCun, Léon Bottou, Yoshua Bengio, and Patrick Haffner. Gradient-based learning applied to document recognition. *Proceedings of the IEEE*, 86(11):2278–2324, 1998.
- [38] Junnan Li, Dongxu Li, Caiming Xiong, and Steven Hoi. Blip: Bootstrapping language-image pre-training for unified vision-language understanding and generation. In *International conference on machine learning*, pages 12888–12900. PMLR, 2022.
- [39] Tsung-Yi Lin, Michael Maire, Serge Belongie, James Hays, Pietro Perona, Deva Ramanan, Piotr Dollár, and C Lawrence Zitnick. Microsoft coco: Common objects in context. In *Computer Vision–ECCV 2014: 13th European Conference, Zurich, Switzerland, September 6–12, 2014, Proceedings, Part V 13*, pages 740–755. Springer, 2014.
- [40] Pantelis Linardatos, Vasilis Papastefanopoulos, and Sotiris Kotsiantis. Explainable ai: A review of machine learning interpretability methods. *Entropy*, 23(1):18, 2020.
- [41] Scott M Lundberg and Su-In Lee. A unified approach to interpreting model predictions. *Advances in neural information processing systems*, 30, 2017.
- [42] Jan Macdonald, Stephan Wäldchen, Sascha Hauch, and Gitta Kutyniok. A rate-distortion framework for explaining neural network decisions. *arXiv preprint arXiv:1905.11092*, 2019.
- [43] Ricardo Moreira, Jacopo Bono, Mário Cardoso, Pedro Saleiro, Mário AT Figueiredo, and Pedro Bizarro. Diconstruct: Causal concept-based explanations through black-box distillation. *arXiv preprint arXiv:2401.08534*, 2024.

- [44] Alfred Müller. Integral probability metrics and their generating classes of functions. *Advances in applied probability*, 29(2):429–443, 1997.
- [45] Tuomas Oikarinen and Tsui-Wei Weng. Clip-dissect: Automatic description of neuron representations in deep vision networks. *arXiv preprint arXiv:2204.10965*, 2022.
- [46] Tuomas Oikarinen, Subhro Das, Lam M Nguyen, and Tsui-Wei Weng. Label-free concept bottleneck models. *arXiv preprint arXiv:2304.06129*, 2023.
- [47] Junhyung Park and Krikamol Muandet. A measure-theoretic approach to kernel conditional mean embeddings. *Advances in neural information processing systems*, 33:21247–21259, 2020.
- [48] Aleksandr Podkopaev, Patrick Blöbaum, Shiva Kasiviswanathan, and Aaditya Ramdas. Sequential kernelized independence testing. In *International Conference on Machine Learning*, pages 27957–27993. PMLR, 2023.
- [49] Alec Radford, Jong Wook Kim, Chris Hallacy, Aditya Ramesh, Gabriel Goh, Sandhini Agarwal, Girish Sastry, Amanda Askell, Pamela Mishkin, Jack Clark, et al. Learning transferable visual models from natural language supervision. In *International conference on machine learning*, pages 8748–8763. PMLR, 2021.
- [50] Vikram V Ramaswamy, Sunnie SY Kim, Ruth Fong, and Olga Russakovsky. Overlooked factors in concept-based explanations: Dataset choice, concept learnability, and human capability. In *Proceedings of the IEEE/CVF Conference on Computer Vision and Pattern Recognition*, pages 10932–10941, 2023.
- [51] Marco Tulio Ribeiro, Sameer Singh, and Carlos Guestrin. " why should i trust you?" explaining the predictions of any classifier. In *Proceedings of the 22nd ACM SIGKDD international conference on knowledge discovery and data mining*, pages 1135–1144, 2016.
- [52] Cynthia Rudin. Stop explaining black box machine learning models for high stakes decisions and use interpretable models instead. *Nature machine intelligence*, 1(5):206–215, 2019.
- [53] Numair Sani, Daniel Malinsky, and Ilya Shpitser. Explaining the behavior of black-box prediction algorithms with causal learning. *arXiv preprint arXiv:2006.02482*, 2020.
- [54] David W Scott. *Multivariate density estimation: theory, practice, and visualization*. John Wiley & Sons, 2015.
- [55] Ramprasaath R Selvaraju, Michael Cogswell, Abhishek Das, Ramakrishna Vedantam, Devi Parikh, and Dhruv Batra. Grad-cam: Visual explanations from deep networks via gradient-based localization. In *Proceedings of the IEEE international conference on computer vision*, pages 618–626, 2017.
- [56] Shalev Shaer, Gal Maman, and Yaniv Romano. Model-x sequential testing for conditional independence via testing by betting. In *International Conference on Artificial Intelligence and Statistics*, pages 2054–2086. PMLR, 2023.
- [57] Glenn Shafer. Testing by betting: A strategy for statistical and scientific communication. *Journal of the Royal Statistical Society Series A: Statistics in Society*, 184(2):407–431, 2021.
- [58] Glenn Shafer and Vladimir Vovk. *Game-theoretic foundations for probability and finance*, volume 455. John Wiley & Sons, 2019.
- [59] John Shawe-Taylor and Nello Cristianini. *Kernel methods for pattern analysis*. Cambridge university press, 2004.

- [60] Shubhanshu Shekhar and Aaditya Ramdas. Nonparametric two-sample testing by betting. *IEEE Transactions on Information Theory*, 2023.
- [61] Tianhong Sheng and Bharath K Sriperumbudur. On distance and kernel measures of conditional dependence. *Journal of Machine Learning Research*, 24(7):1–16, 2023.
- [62] Pushkar Shukla, Sushil Bharati, and Matthew Turk. Cavli-using image associations to produce local concept-based explanations. In *Proceedings of the IEEE/CVF Conference on Computer Vision and Pattern Recognition*, pages 3749–3754, 2023.
- [63] Amanpreet Singh, Ronghang Hu, Vedanuj Goswami, Guillaume Couairon, Wojciech Galuba, Marcus Rohrbach, and Douwe Kiela. Flava: A foundational language and vision alignment model. In *Proceedings of the IEEE/CVF Conference on Computer Vision and Pattern Recognition*, pages 15638–15650, 2022.
- [64] Le Song, Jonathan Huang, Alex Smola, and Kenji Fukumizu. Hilbert space embeddings of conditional distributions with applications to dynamical systems. In *Proceedings of the 26th Annual International Conference on Machine Learning*, pages 961–968, 2009.
- [65] Bharath K Sriperumbudur, Arthur Gretton, Kenji Fukumizu, Bernhard Schölkopf, and Gert RG Lanckriet. Hilbert space embeddings and metrics on probability measures. *The Journal of Machine Learning Research*, 11:1517–1561, 2010.
- [66] Wesley Tansey, Victor Veitch, Haoran Zhang, Raul Rabadan, and David M Blei. The holdout randomization test for feature selection in black box models. *Journal of Computational and Graphical Statistics*, 31(1):151–162, 2022.
- [67] Jacopo Teneggi, Alexandre Luster, and Jeremias Sulam. Fast hierarchical games for image explanations. *IEEE Transactions on Pattern Analysis and Machine Intelligence*, 45(4):4494–4503, 2022.
- [68] Jacopo Teneggi, Beepul Bharti, Yaniv Romano, and Jeremias Sulam. Shap-xrt: The shapley value meets conditional independence testing. *Transactions on Machine Learning Research*, 2023.
- [69] Isabella Verdinelli and Larry Wasserman. Feature importance: A closer look at shapley values and loco. *arXiv preprint arXiv:2303.05981*, 2023.
- [70] Isabella Verdinelli and Larry Wasserman. Decorrelated variable importance. *Journal of Machine Learning Research*, 25(7):1–27, 2024.
- [71] Sebastiano Vigna. A weighted correlation index for rankings with ties. In *Proceedings of the 24th international conference on World Wide Web*, pages 1166–1176, 2015.
- [72] Jean Ville. *Etude critique de la notion de collectif*. Gauthier-Villars Paris, 1939.
- [73] Vladimir Vovk and Ruodu Wang. E-values: Calibration, combination and applications. *The Annals of Statistics*, 49(3):1736–1754, 2021.
- [74] Catherine Wah, Steve Branson, Peter Welinder, Pietro Perona, and Serge Belongie. The caltech-ucsd birds-200-2011 dataset. 2011.
- [75] Benyou Wang, Qianqian Xie, Jiahuan Pei, Zhihong Chen, Prayag Tiwari, Zhao Li, and Jie Fu. Pre-trained language models in biomedical domain: A systematic survey. *ACM Computing Surveys*, 56(3): 1–52, 2023.

- [76] Ruodu Wang and Aaditya Ramdas. False discovery rate control with e-values. *Journal of the Royal Statistical Society Series B: Statistical Methodology*, 84(3):822–852, 2022.
- [77] Zifeng Wang, Zhenbang Wu, Dinesh Agarwal, and Jimeng Sun. Medclip: Contrastive learning from unpaired medical images and text. *arXiv preprint arXiv:2210.10163*, 2022.
- [78] Shirley Wu, Mert Yuksekgonul, Linjun Zhang, and James Zou. Discover and cure: Concept-aware mitigation of spurious correlation. In *International Conference on Machine Learning*, pages 37765–37786. PMLR, 2023.
- [79] Yongqin Xian, Christoph H Lampert, Bernt Schiele, and Zeynep Akata. Zero-shot learning—a comprehensive evaluation of the good, the bad and the ugly. *IEEE transactions on pattern analysis and machine intelligence*, 41(9):2251–2265, 2018.
- [80] Yue Yang, Artemis Panagopoulou, Shenghao Zhou, Daniel Jin, Chris Callison-Burch, and Mark Yatskar. Language in a bottle: Language model guided concept bottlenecks for interpretable image classification. In *Proceedings of the IEEE/CVF Conference on Computer Vision and Pattern Recognition*, pages 19187–19197, 2023.
- [81] Hao Yuan, Haiyang Yu, Shurui Gui, and Shuiwang Ji. Explainability in graph neural networks: A taxonomic survey. *IEEE transactions on pattern analysis and machine intelligence*, 45(5):5782–5799, 2022.
- [82] Mert Yuksekgonul, Maggie Wang, and James Zou. Post-hoc concept bottleneck models. *arXiv preprint arXiv:2205.15480*, 2022.
- [83] Kun Zhang, Jonas Peters, Dominik Janzing, and Bernhard Schölkopf. Kernel-based conditional independence test and application in causal discovery. *arXiv preprint arXiv:1202.3775*, 2012.

## A Testing by Betting

In this appendix, we include additional background information on testing by betting that was omitted from the main text for the sake of conciseness of presentation.

Recall that the wealth process  $\{K_t\}_{t \in \mathbb{N}_0}$  with  $\mathbb{N}_0 := \mathbb{N} \cup \{0\}$  is defined as

$$K_0 = 1 \quad \text{and} \quad K_t = K_{t-1} \cdot (1 + v_t \kappa_t) \quad (39)$$

where  $v_t \in [-1, 1]$  is the betting fraction and  $\kappa_t \in [-1, 1]$  the payoff of the bet.

### A.1 Test Martingales

We start by introducing the definition of a *test martingale* (see, for example, Shaer et al. [56]).

**Definition A.1** (Test martingale). A nonnegative stochastic process  $\{S_t\}_{t \in \mathbb{N}_0}$  is a test martingale if  $S_0 = 1$  and, under a null hypothesis  $H_0$ , it is a supermartingale, i.e.

$$\mathbb{E}_{H_0}[S_t \mid \mathcal{F}_{t-1}] \leq S_{t-1}, \quad (40)$$

where  $\mathcal{F}_{t-1}$  is the filtration (i.e., the smallest  $\sigma$ -algebra) of all previous observations.

In the following, we will use Ville's inequality, which we include for the sake of completeness.

**Lemma A.1** (Ville's inequality [72]). *If the stochastic process  $\{S_t\}_{t \in \mathbb{N}_0}$  is a nonnegative supermartingale,*

$$\mathbb{P}[\exists t \geq 0 : S_t \geq \eta] \leq \mathbb{E}[S_0]/\eta, \quad \forall \eta > 0. \quad (41)$$

#### Proof of Lemma 2

Recall the lemma states that if

$$\mathbb{E}_{H_0}[\kappa_t \mid \mathcal{F}_{t-1}] = 0 \quad (42)$$

then

$$\mathbb{P}_{H_0}[\exists t \geq 1 : K_t \geq 1/\alpha] \leq \alpha, \quad (43)$$

i.e. we can use the wealth process to reject the null hypothesis  $H_0$  with Type I error control.

*Proof.* It suffices to show that if  $\mathbb{E}_{H_0}[\kappa_t \mid \mathcal{F}_{t-1}] = 0$ , then the wealth process  $\{K_t\}_{t \in \mathbb{N}_0}$  is a test martingale:

1.  $K_0 = 1$  by definition, and
2. It is immediate to see that the wealth process is nonnegative because  $v_t \kappa_t \in [-1, 1]$  and the bettor never risks more than their current wealth, i.e. they will never go into debt. Finally,
3. If  $\mathbb{E}_{H_0}[\kappa_t \mid \mathcal{F}_{t-1}] = 0$ , then

$$\mathbb{E}_{H_0}[K_t \mid \mathcal{F}_{t-1}] = \mathbb{E}_{H_0}[K_{t-1} \cdot (1 + v_t \kappa_t) \mid \mathcal{F}_{t-1}] \quad (44)$$

$$= K_{t-1} \cdot \mathbb{E}_{H_0}[1 + v_t \kappa_t \mid \mathcal{F}_{t-1}] \quad (K_{t-1} \mid \mathcal{F}_{t-1} \text{ is constant}) \quad (45)$$

$$\leq K_{t-1} \cdot (1 + \mathbb{E}_{H_0}[\kappa_t \mid \mathcal{F}_{t-1}]) \quad (v_t \leq 1) \quad (46)$$

$$= K_{t-1}, \quad (47)$$

and the wealth process is a supermartingale under the null.

Then, by Ville's inequality, we conclude that for any significance level  $\alpha \in (0, 1)$

$$\mathbb{P}_{H_0}[\exists t \geq 1 : K_t \geq 1/\alpha] \leq \alpha \mathbb{E}[K_0] = \alpha \quad (48)$$

which is the statement of the proposition.  $\square$

## A.2 Symmetry-based Two-sample Sequential Testing

In this section, we show how to leverage symmetry to construct valid sequential tests for a two-sample null hypothesis of the form

$$H_0 : P = \tilde{P}. \quad (49)$$

**Lemma A.2** (See [48, 56, 60]).  $\forall t \geq 1$ , let  $X \sim P$  and  $\tilde{X} \sim \tilde{P}$  be two random variables sampled from  $P$  and  $\tilde{P}$ , respectively. If  $P = \tilde{P}$ , it holds that for any fixed function  $\rho_t : \mathcal{X} \rightarrow \mathbb{R}$

$$\rho_t(X) - \rho_t(\tilde{X}) \stackrel{d}{=} \rho_t(\tilde{X}) - \rho_t(X), \quad (50)$$

that is

$$p_0(\rho_t(X) - \rho_t(\tilde{X})) = p_0(\rho_t(\tilde{X}) - \rho_t(X)), \quad (51)$$

where  $p_0$  is the probability density function induced by  $H_0$ .

*Proof.* The proof is straightforward. If  $P = \tilde{P}$ , then  $X$  and  $\tilde{X}$  are exchangeable by assumption.  $\square$

### Proof of Lemma 3

Recall the lemma states that for any fixed function  $\rho_t : \mathcal{X} \rightarrow \mathbb{R}$ , the payoff

$$\kappa_t = \tanh(\rho_t(X) - \rho_t(\tilde{X})) \quad (52)$$

provides a fair game (i.e., it satisfies Lemma 2) for a two-sample test with null hypothesis  $H_0 : P = \tilde{P}$ . We use Lemma A.2 above to prove a stronger result that implies the desired claim.

**Lemma A.3** (See [48, 56, 60]). For any  $t \geq 1$ , and any fixed anti-symmetric function  $\xi : \mathbb{R} \rightarrow \mathbb{R}$ , it holds that

$$\mathbb{E}_{H_0}[\xi(\rho_t(X) - \rho_t(\tilde{X})) \mid \mathcal{F}_{t-1}] = 0. \quad (53)$$

*Proof.* We can see that

$$\mathbb{E}_{H_0}[\xi(\rho_t(X) - \rho_t(\tilde{X})) \mid \mathcal{F}_{t-1}] = \mathbb{E}_{H_0}[\xi(\rho_t(X) - \rho_t(\tilde{X}))] \quad (\rho_t, \xi \text{ are fixed}) \quad (54)$$

$$= \int_{\mathbb{R}} \xi(u) p_0(u) \, du \quad (\text{change of variables}) \quad (55)$$

$$= \int_{\mathbb{R}_+} (\xi(u) + \xi(-u)) p_0(u) \, du \quad (\text{by Lemma A.2}) \quad (56)$$

$$= \int_{\mathbb{R}_+} (\xi(u) - \xi(u)) p_0(u) \, du \quad (\xi \text{ is anti-symmetric}) \quad (57)$$

$$= 0, \quad (58)$$

which concludes the proof.  $\square$

*Proof of Lemma 3.* First note that  $\tanh$  is an anti-symmetric function, so Lemma A.3 holds. Then, Lemma 2 implies that  $\kappa_t = \tanh(\rho_t(X) - \rho_t(\tilde{X}))$  provides a test martingale for  $H_0 : P = \tilde{P}$ .  $\square$

## A.3 Betting Strategies

So far, we have discussed how to construct valid test martingales in terms of the payoff  $\kappa_t$ . Then, it remains to define a strategy to choose the betting fraction  $v_t$ . In general, any method that picks  $v_t$  *before* data is revealed maintains validity of the test, and we briefly summarize a few alternatives.



**Constant betting fraction.** Naturally, a fixed betting fraction  $v_t = v$  is valid. However, this strategy may be prone to *overshooting*, i.e. the wealth may go to zero almost surely under the alternative, and severely impact the power of the test [48, Example 2].

**Mixture method** [16, 56]. A possible way to overcome the limitations of setting a fixed betting fraction is to average across a distribution, i.e.

$$K_t = \int_{\mathcal{V}} K_t^{(v)} p(v) \, dv, \quad (59)$$

where  $K_t^{(v)}$  is the wealth with betting fraction  $v$ , and  $p(v)$  is a prior (e.g., uniform over  $[0, 1]$ ). This choice is valid, and motivated by the intuition that the mixture martingale will be driven by the term that achieves the optimal betting fraction [56, Theorem 1].

**Online Newton step (ONS)** [18]. Alternatively, one can frame choosing the betting fraction as an online optimization problem that finds the optimal  $v_t$  in terms of the regret of the strategy. We refer interested readers to [18, 56, 60] for a theoretical analysis of this strategy and simply state here the wealth’s rate of growth. Algorithm A.1 summarizes this strategy.

**Lemma A.4** (See Shekhar and Ramdas [60]). *For any sequence  $\{v_t \in [-1, 1] : t \geq 1\}$ , it holds that*

$$\log K_t \geq \frac{1}{8t} \left( \sum_{t'=1}^t v_{t'} \right)^2 - \log t. \quad (60)$$

---

#### Algorithm A.1 ONS Betting Strategy

---

**Input:** Sequence of payoffs  $\{\kappa_t\}_{t \geq 1}$

- 1:  $a_0 \leftarrow 1$
  - 2:  $v_1 \leftarrow 0$
  - 3: **for**  $t \geq 1$  **do**
  - 4:    $z_t \leftarrow \kappa_t / (1 + v_t \kappa_t)$
  - 5:    $a_t \leftarrow a_{t-1} + z_t^2$
  - 6:    $v_{t+1} \leftarrow \max(0, \min(1, a_t + 2/(2 - \log(3)) \cdot z_t/a_t))$
  - 7: **end for**
- 

## B Technical Details on Payoff Functions

In this appendix, we include technical details on how to compute the payoff functions of all tests presented in this paper. We start with a brief overview of the maximum mean discrepancy (MMD) [28], and we refer interested readers to [1, 4, 59, 65] for rigorous introductions to the theory of reproducing kernel Hilbert spaces (RKHSs) and their applications to probability and statistics.

**Definition B.2** (Mean embedding (see Gretton et al. [28])). Let  $P$  be a probability distribution on  $\mathcal{X}$  and  $\mathcal{R}$  an RKHS on the same domain. The mean embedding of  $P$  in  $\mathcal{R}$  is the element  $\mu_P \in \mathcal{R}$  such that

$$\forall \rho \in \mathcal{R}, \mathbb{E}_P[\rho(X)] = \langle \mu_P, \rho \rangle_{\mathcal{R}}. \quad (61)$$

Furthermore, given  $X^{(1)}, \dots, X^{(n)}$  sampled i.i.d. from  $P$ , the plug-in estimate  $\hat{\mu}_P^{(n)}$  is

$$\hat{\mu}_P^{(n)} := \frac{1}{n} \sum_{i=1}^n \varphi(X^{(i)}), \quad (62)$$

where  $\varphi$  is the canonical feature map, i.e.  $\varphi(X) = k(X, \cdot)$ , and  $k$  is the kernel associated with  $\mathcal{R}$ .

We now define the MMD between two probability distributions  $P, Q$  and show that it can be rewritten in terms of their mean embeddings.

**Definition B.3** (Integral probability metric (see Müller [44])). Let  $P, Q$  be two probability distributions over  $\mathcal{X}$ . Furthermore, denote  $\mathcal{G} = \{g : \mathcal{X} \rightarrow \mathbb{R}\}$  a hypothesis class of real-valued functions over  $\mathcal{X}$ . Then,

$$D_{\mathcal{G}}(P, Q) := \sup_{g \in \mathcal{G}} |\mathbb{E}_P[g(X)] - \mathbb{E}_Q[g(X)]| \quad (63)$$

is the distance between  $P$  and  $Q$  induced by  $\mathcal{G}$ , and the function  $g^*$  that achieves the supremum is called *witness function*.

The MMD is defined as  $D_{\mathcal{B}(\mathcal{R})}(P, Q)$ , where  $\mathcal{B}(\mathcal{R})$  is the unit ball of  $\mathcal{R}$ , i.e.

$$\mathcal{B}(\mathcal{R}) := \{\rho \in \mathcal{R} : \|\rho\|_{\mathcal{R}} \leq 1\}. \quad (64)$$

**Definition B.4** (Maximum mean discrepancy (see Gretton et al. [28])). For  $P, Q$  defined as above, let  $\mathcal{R}$  be an RKHS on their domain. Then,

$$\text{MMD}(P, Q) := \sup_{\rho \in \mathcal{B}(\mathcal{R})} |\mathbb{E}_P[\rho(X)] - \mathbb{E}_Q[\rho(X)]|. \quad (65)$$

We note that we drop the absolute value because if  $\rho \in \mathcal{B}(\mathcal{R})$ , then  $-\rho \in \mathcal{B}(\mathcal{R})$  also. From the definition of mean embedding, it follows that

$$\text{MMD}(P, Q) = \sup_{\rho \in \mathcal{B}(\mathcal{R})} \langle \rho, \mu_P \rangle_{\mathcal{R}} - \langle \rho, \mu_Q \rangle_{\mathcal{R}} = \frac{\|\mu_P - \mu_Q\|_{\mathcal{R}}}{\|\mu_P - \mu_Q\|_{\mathcal{R}}}, \quad (66)$$

and its witness function satisfies

$$\rho^* \propto \mu_P - \mu_Q. \quad (67)$$

## B.1 Computing $\rho_t^{\text{SKIT}}$

Recall that  $\rho_t^{\text{SKIT}}$  is the estimate of  $\text{MMD}(P_{\hat{Y}Z_j}, P_{\hat{Y}} \times P_{Z_j})$  at time  $t$ , i.e.

$$\rho_t^{\text{SKIT}} = \hat{\mu}_{\hat{Y}Z_j}^{(2(t-1))} - \hat{\mu}_{\hat{Y}}^{(2(t-1))} \otimes \hat{\mu}_{Z_j}^{(2(t-1))}, \quad (68)$$

where

$$\hat{\mu}_{\hat{Y}Z_j}^{(2(t-1))} = \frac{1}{2(t-1)} \sum_{t'=0}^{2(t-1)} (\varphi_{\hat{Y}}(\hat{Y}^{(t')}) \otimes \varphi_{Z_j}(Z_j^{(t')})), \quad (69)$$

$$\hat{\mu}_{\hat{Y}}^{(2(t-1))} = \frac{1}{t-1} \sum_{t'=0}^{2(t-1)} \varphi_{\hat{Y}}(\hat{Y}^{(t')}), \quad \hat{\mu}_{Z_j}^{(2(t-1))} = \frac{1}{t-1} \sum_{t'=0}^{2(t-1)} \varphi_{Z_j}(Z_j^{(t')}), \quad (70)$$

and  $\varphi_{\hat{Y}}, \varphi_{Z_j}$  are the canonical feature maps associated with  $\mathcal{R}_{\hat{Y}}$  and  $\mathcal{R}_{Z_j}$ , respectively. We remark that  $\rho_t^{\text{SKIT}}$  is an operator, and, for a sample  $(\hat{y}, z_j)$ , its value  $\rho_t^{\text{SKIT}}(\hat{y}, z_j)$  can be computed as

$$\rho_t^{\text{SKIT}}(\hat{y}, z_j) = (\hat{\mu}_{\hat{Y}Z_j}^{(2(t-1))} - \hat{\mu}_{\hat{Y}}^{(2(t-1))} \otimes \hat{\mu}_{Z_j}^{(2(t-1))})(\hat{y}, z_j) \quad (71)$$

$$= \hat{\mu}_{\hat{Y}Z_j}^{(2(t-1))}(\hat{y}, z_j) - (\hat{\mu}_{\hat{Y}}^{(2(t-1))} \otimes \hat{\mu}_{Z_j}^{(2(t-1))})(\hat{y}, z_j) \quad (72)$$

with

$$\hat{\mu}_{\hat{Y}Z_j}^{(2(t-1))}(\hat{y}, z_j) = \frac{1}{2(t-1)} \sum_{t'=0}^{2(t-1)} k_{\hat{Y}}(\hat{Y}^{(t')}, \hat{y}) k_{Z_j}(Z_j^{(t')}, z_j) \quad (73)$$

$$(\hat{\mu}_{\hat{Y}}^{(2(t-1))} \otimes \hat{\mu}_{Z_j}^{(2(t-1))})(\hat{y}, z_j) = \frac{1}{2(t-1)} \sum_{t'=0}^{2(t-1)} k_{\hat{Y}}(\hat{Y}^{(t')}, \hat{y}) \cdot \frac{1}{2(t-1)} \sum_{t''=0}^{2(t-1)} k_{Z_j}(Z_j^{(t'')}, z_j), \quad (74)$$

where  $k_{\hat{Y}}, k_{Z_j}$  are the kernels associated with  $\mathcal{R}_{\hat{Y}}$  and  $\mathcal{R}_{Z_j}$ , respectively.

## B.2 Computing $\rho_t^{\text{c-SKIT}}$

Recall that  $\rho_t^{\text{c-SKIT}}$  is the estimate of  $\text{MMD}(P_{\hat{Y}Z_jZ_{-j}}, P_{\hat{Y}\tilde{Z}_jZ_{-j}})$  with  $\tilde{Z}_j \sim P_{Z_j|Z_{-j}}$  at time  $t$ , i.e.

$$\rho_t^{\text{c-SKIT}} = \hat{\mu}_{\hat{Y}Z_jZ_{-j}}^{(t-1)} - \hat{\mu}_{\hat{Y}\tilde{Z}_jZ_{-j}}^{(t-1)}, \quad (75)$$

where

$$\hat{\mu}_{\hat{Y}Z_jZ_{-j}}^{(t-1)} = \frac{1}{t-1} \sum_{t'=0}^{t-1} \left( \varphi_{\hat{Y}}(\hat{Y}^{(t')}) \otimes \varphi_{Z_j}(Z_j^{(t')}) \otimes \varphi_{Z_{-j}}(Z_{-j}^{(t')}) \right) \quad (76)$$

$$\hat{\mu}_{\hat{Y}\tilde{Z}_jZ_{-j}}^{(t-1)} = \frac{1}{t-1} \sum_{t'=0}^{t-1} \left( \varphi_{\hat{Y}}(\hat{Y}^{(t')}) \otimes \varphi_{Z_j}(\tilde{Z}_j^{(t')}) \otimes \varphi_{Z_{-j}}(Z_{-j}^{(t')}) \right) \quad (77)$$

and  $\varphi_{\hat{Y}}, \varphi_{Z_j}, \varphi_{Z_{-j}}$  are the canonical feature maps associated with their respective RKHSs. We remark that  $\rho_t^{\text{c-SKIT}}$  is defined as an operator, and, for a triplet  $(\hat{y}, z_j, z_{-j})$  its value can be computed as

$$\rho_t^{\text{c-SKIT}}(\hat{y}, z_j, z_{-j}) = (\hat{\mu}_{\hat{Y}Z_jZ_{-j}}^{(t-1)} - \hat{\mu}_{\hat{Y}\tilde{Z}_jZ_{-j}}^{(t-1)})(\hat{y}, z_j, z_{-j}) \quad (78)$$

$$= \hat{\mu}_{\hat{Y}Z_jZ_{-j}}^{(t-1)}(\hat{y}, z_j, z_{-j}) - \hat{\mu}_{\hat{Y}\tilde{Z}_jZ_{-j}}^{(t-1)}(\hat{y}, z_j, z_{-j}) \quad (79)$$

with

$$\hat{\mu}_{\hat{Y}Z_jZ_{-j}}^{(t-1)}(\hat{y}, z_j, z_{-j}) = \frac{1}{t-1} \sum_{t'=0}^{t-1} k_{\hat{Y}}(\hat{Y}^{(t')}, \hat{y}) k_{Z_j}(Z_j^{(t')}, z_j) k_{Z_{-j}}(Z_{-j}^{(t')}, z_{-j}) \quad (80)$$

$$\hat{\mu}_{\hat{Y}\tilde{Z}_jZ_{-j}}^{(t-1)}(\hat{y}, z_j, z_{-j}) = \frac{1}{t-1} \sum_{t'=0}^{t-1} k_{\hat{Y}}(\hat{Y}^{(t')}, \hat{y}) k_{Z_j}(\tilde{Z}_j^{(t')}, z_j) k_{Z_{-j}}(Z_{-j}^{(t')}, z_{-j}) \quad (81)$$

where  $k_{\hat{Y}}, k_{Z_j}, k_{Z_{-j}}$  are the kernels associated with  $\mathcal{R}_{\hat{Y}}, \mathcal{R}_{Z_j}$ , and  $\mathcal{R}_{Z_{-j}}$ , respectively.

### B.3 Computing $\rho_t^{\text{x-SKIT}}$

Recall that, for a particular sample  $z$ , a concept  $j \in [m]$ , and a subset  $S \subseteq [m] \setminus \{j\}$  that does not contain  $j$ ,  $\rho_t^{\text{x-SKIT}}$  is the estimate—at time  $t$ —of  $\text{MMD}(\hat{Y}_{S \cup \{j\}}, \hat{Y}_S)$  with  $\hat{Y}_C = g(\hat{H}_C)$ ,  $\hat{H}_C \sim P_{H|Z_C=z_C}$ , i.e.

$$\rho_t^{\text{x-SKIT}} = \hat{\mu}_{\hat{Y}_{S \cup \{j\}}}^{(t-1)} - \hat{\mu}_{\hat{Y}_S}^{(t-1)}, \quad (82)$$

where

$$\hat{\mu}_{\hat{Y}_{S \cup \{j\}}}^{(t-1)} = \frac{1}{t-1} \sum_{t'=0}^{t-1} \varphi_{\hat{Y}}(\hat{Y}_{S \cup \{j\}}^{(t')}), \quad \hat{\mu}_{\hat{Y}_S}^{(t-1)} = \frac{1}{t-1} \sum_{t'=0}^{t-1} \varphi_{\hat{Y}}(\hat{Y}_S^{(t')}), \quad (83)$$

and  $\varphi_{\hat{Y}}$  is the canonical feature map of  $\mathcal{R}_{\hat{Y}}$ . Then, for a prediction  $\hat{y}$ , the value of  $\rho_t^{\text{x-SKIT}}$  is

$$\rho_t^{\text{x-SKIT}}(\hat{y}) = (\hat{\mu}_{\hat{Y}_{S \cup \{j\}}}^{(t-1)} - \hat{\mu}_{\hat{Y}_S}^{(t-1)})(\hat{y}) \quad (84)$$

$$= \hat{\mu}_{\hat{Y}_{S \cup \{j\}}}^{(t-1)}(\hat{y}) - \hat{\mu}_{\hat{Y}_S}^{(t-1)}(\hat{y}) \quad (85)$$

$$= \frac{1}{t-1} \sum_{t'=0}^{t-1} k_{\hat{Y}}(\hat{Y}_{S \cup \{j\}}^{(t')}, \hat{y}) - \frac{1}{t-1} \sum_{t'=0}^{t-1} k_{\hat{Y}}(\hat{Y}_S^{(t')}, \hat{y}), \quad (86)$$

where  $k_{\hat{Y}}$  is the kernel associated with  $\mathcal{R}_{\hat{Y}}$ .

## C Proofs

In this appendix, we include the proofs of the results presented in this paper.

### C.1 Proof of Lemma 1

Recall that  $c \in \mathbb{R}^{d \times m}$  is a dictionary of  $m$  concepts such that  $c_j$ ,  $j \in [m]$  is the vector representation of the  $j^{\text{th}}$  concept. Then,  $Z = \langle c, H \rangle$  is the vector such that—with appropriate normalization— $Z_j \in [-1, 1]$  represents the amount of concept  $j$  in  $h$ .

We want to show that if  $\hat{Y} = \langle w, H \rangle$ ,  $w \in \mathbb{R}^d$ , and  $d \geq 3$ , then

$$\hat{Y} \perp\!\!\!\perp Z_j \iff \langle w, c_j \rangle = 0. \quad (87)$$

That is,  $w$  being orthogonal to  $c_j$  does not provide any information about the statistical dependence between  $\hat{Y}$  and  $Z_j$ , and vice versa.

*Proof.* Herein, for the sake of simplicity, we will drop the  $c_j$  notation and consider a single concept  $c$ . Furthermore, we will assume that all vectors are normalized, i.e.  $\|w\| = \|h\| = \|c\| = 1$ . Note that the Eq. (87) above can directly be rewritten as

$$\langle w, H \rangle \perp\!\!\!\perp \langle c, H \rangle \iff \langle w, c \rangle = 0. \quad (88)$$

( $\iff$ ) We show there exist random vectors  $H$  such that  $\langle w, c \rangle = 0$  but  $\langle w, H \rangle \not\perp\!\!\!\perp \langle c, H \rangle$ .

Let  $H \sim \mathcal{U}(\mathbb{S}^d)$ , i.e.  $H = [H_1, \dots, H_d]$  is sampled uniformly over the sphere in  $d$  dimensions. It is easy to see that  $\forall j \in [d]$ ,  $H_j = \langle e_j, H \rangle$ , where  $e_j$  is the  $j^{\text{th}}$  element of the standard basis. Furthermore, it holds that  $H_j = \sqrt{1 - \sum_{j' \neq j} H_{j'}^2}$  by definition. We conclude that  $\forall (j, j')$ , let  $w = e_j$  and  $c = e_{j'}$ , then  $\langle w, c \rangle = 0$  but  $\langle w, H \rangle \not\perp\!\!\!\perp \langle c, H \rangle$ . That is, the fact that  $e_j$  and  $e_{j'}$  are orthogonal does not mean that their respective projections of  $H$  are statistically independent.

( $\Rightarrow$ ) We show how to construct a random vector  $H$  such that  $\langle w, H \rangle \perp \langle c, H \rangle$  but  $\langle w, c \rangle \neq 0$ .

Denote  $\mathcal{H}_\eta := \{h \in \mathbb{S}^d : \langle c, h \rangle = \eta, \eta \neq 0\}$  the linear subspace of unit vectors in  $\mathbb{R}^d$  with the same nonzero inner product with  $c$ . Each vector  $h \in \mathcal{H}_\eta$  can be decomposed into a parallel and an orthogonal component to  $c$ , i.e.  $\forall h \in \mathcal{H}_\eta, h = h_c + h_\perp = \eta c + h_\perp$ , where the last equality follows by definition of  $\mathcal{H}_\eta$ .

Consider  $\mathcal{H}_\eta$  and  $\mathcal{H}_{-\eta}$ , it follows that for  $w, h^+ \in \mathcal{H}_\eta$  and  $h^- \in \mathcal{H}_{-\eta}$

$$\langle w, h^+ \rangle = \langle w, h^- \rangle \iff \langle \eta c + w_\perp, \eta c + h_\perp^+ \rangle = \langle \eta c + w_\perp, -\eta c + h_\perp^- \rangle \quad (89)$$

$$\iff \eta^2 + \langle w_\perp, h_\perp^+ \rangle = -\eta^2 + \langle w_\perp, h_\perp^- \rangle \quad (90)$$

$$\iff \langle w_\perp, h_\perp^+ - h_\perp^- \rangle = -2\eta^2 \quad (91)$$

$$\iff \langle w_\perp, \Delta \rangle = -2\eta^2. \quad (\Delta := h_\perp^+ - h_\perp^-) \quad (92)$$

Denote  $\mathcal{S} = \{(h^+, h^-) : \langle w_\perp, \Delta \rangle = -2\eta^2\}$  the set of pairs of vector that satisfy Eq. (92), and note that for each pair  $(h^+, h^-)$  there exists a value  $\beta$  such that  $\langle w, h^+ \rangle = \langle w, h^- \rangle = \beta$ . Then, sampling from  $\mathcal{S}$  is equivalent to sampling from the set of possible correlations with  $w$  that can be attained by vectors both in  $\mathcal{H}_\eta$  and  $\mathcal{H}_{-\eta}$ .

Note that when  $d = 2$ ,  $h_\perp^+, h_\perp^- \in \{\pm w_\perp\}$  by construction, hence  $\Delta \in \{0, \pm 2w_\perp\}$  and  $\langle w_\perp, \Delta \rangle \in \{0, \pm 2(1 - \eta^2)\}$ . Then,  $\mathcal{S} = \emptyset$  because there are no pairs of vectors such that  $\langle w_\perp, \Delta \rangle = -2\eta^2$ . For  $d \geq 3$ ,  $\mathcal{S}$  is nonempty as long as  $\eta \leq \sqrt{1/2}$ .

Then, we can construct  $H$  as follows:

- Sample the component parallel to  $c$ , i.e.  $H_c \sim \mathcal{U}(\pm \eta c)$ ,
- Sample the component orthogonal to  $c$ , i.e.  $(H_\perp^+, H_\perp^-) \sim \mathcal{U}(\mathcal{S})$ ,

and note that by doing so, we have sampled  $\langle c, H \rangle$  and  $\langle w, H \rangle$  independently. Finally

$$H = \begin{cases} H_c + H_\perp^+ & \text{if } H_c = \eta c \\ H_c + H_\perp^- & \text{if } H_c = -\eta c \end{cases} \quad (93)$$

has  $\langle w, H \rangle \perp \langle c, H \rangle$  by construction, but, since  $w \in \mathcal{H}_\eta$ ,  $\langle w, c \rangle = \eta \neq 0$ .

This concludes the proof of the lemma.  $\square$

## C.2 Proof of Proposition 1

Recall that Proposition 1 states that the payoff function

$$\kappa_t^{\text{c-SKIT}} = \tanh(\rho_t^{\text{c-SKIT}}(\hat{Y}, Z_j, Z_{-j}) - \rho_t^{\text{c-SKIT}}(\hat{Y}, \tilde{Z}_j, Z_{-j})) \quad (94)$$

provides a fair game for the global conditional semantic importance null hypothesis  $H_{0,j}^{\text{GC}}$  in Definition 2. That is, the wealth process provides Type I error control.

*Proof.* Note that  $H_{0,j}^{\text{GC}}$  can be directly rewritten as

$$H_{0,j}^{\text{GC}} : P_{\hat{Y} Z_j Z_{-j}} = P_{\hat{Y} \tilde{Z}_j Z_{-j}} \quad (95)$$

where  $\tilde{Z}_j \sim P_{Z_j | Z_{-j}}$ . Then, under the null, the triplets  $(\hat{Y}, Z_j, Z_{-j})$  and  $(\hat{Y}, \tilde{Z}_j, Z_{-j})$  are exchangeable by assumption, and the result follows from Lemma 3.  $\square$

### C.3 Proof of Proposition 2

Recall that Proposition 2 claims that a wealth process with

$$\kappa_t^{\text{x-SKIT}} = \tanh(\rho_t^{\text{x-SKIT}}(\hat{Y}_{S \cup \{j\}}) - \rho_t^{\text{x-SKIT}}(\hat{Y}_S)) \quad (96)$$

can be used to reject the local conditional semantic importance  $H_{0,j,S}^{\text{LC}}$  in Definition 3 with Type I error control, i.e. the game is fair.

*Proof.* It is easy to see that  $H_{0,j,S}^{\text{LC}}$  is already written as a two-sample test. Then, under this null,  $\hat{Y}_{S \cup \{j\}}$  and  $\hat{Y}_S$  are exchangeable by assumption, and Lemma 3 implies the statement of the proposition.  $\square$

## D Experimental Details

In this appendix, we include further details on the real-world data experiments.

### D.1 Estimating Conditional Distributions from Data

Here, we introduce nonparametric methods to estimate the conditional distributions necessary to run our c-SKIT and x-SKIT tests. Throughout this section, we will assume access to a training set  $\{(h^{(i)}, z^{(i)})\}_{i=1}^n$  of  $n$  tuples of dense embeddings  $h \in \mathbb{R}^d$  with their semantics  $z \in [-1, 1]^m$ .

#### D.1.1 Estimating $P_{Z_j|Z_{-j}}$ for c-SKIT

Here, we describe how to sample from the conditional distribution of a concept  $Z_j$  given the rest,  $Z_{-j}$ , i.e.  $\tilde{Z}_j \sim P_{Z_j|Z_{-j}}$ , which is necessary to run our c-SKIT test. In particular, for a concept  $j \in [m]$ , and an observation  $z \in [-1, 1]^m$ , we define the unnormalized conditional distribution

$$\tilde{p}(z_j | z_{-j}) = \sum_{i=1}^n w_i \phi \left( \frac{z_j^{(i)} - z_j}{\nu_{\text{scott}}} \right) \quad (97)$$

by means of weighted kernel density estimation (KDE), where  $\phi$  is the standard normal probability density function,  $\nu_{\text{scott}}$  is Scott's factor [54], and

$$w_i = \phi \left( \frac{z_{-j}^{(i)} - z_{-j}}{\nu} \right), \quad \nu > 0 \quad (98)$$

are the weights. That is, the further  $z_{-j}^{(i)}$  is from  $z_{-j}$ , the lower its weight in the KDE. As for all kernel-based methods, the bandwidth  $\nu$  is important for the practical performance of the model. For our experiments, we choose  $\nu$  adaptively such that the effective number of points in the KDE (i.e.  $n_{\text{eff}} = (\sum_{i=1}^n w_i)^2 / \sum_{i=1}^n w_i^2$ ) is the same across concepts. This choice is motivated by the fact that different concepts have different distributions, and we want to guarantee the same number of points are used to estimate their conditional distributions. Furthermore, we note that  $n_{\text{eff}}$  controls the strength of the conditioning—the larger  $n_{\text{eff}}$ , the slower the decay of the weights, and the weaker the conditioning. That is, in the limit, the weights become uniform, the conditional distribution tends to the marginal  $\tilde{p}(z_j)$ , and all tests presented become of decorrelated semantic importance [69, 70]. With this, sampling  $\tilde{Z}_j \sim P_{Z_j|Z_{-j}=z_{-j}}$  boils down to first sampling  $i'$  according to the weights  $w = [w_1, \dots, w_n]$ , and then sampling  $\tilde{Z}_j$  from the Gaussian distribution centered at  $z_j^{(i')}$ .



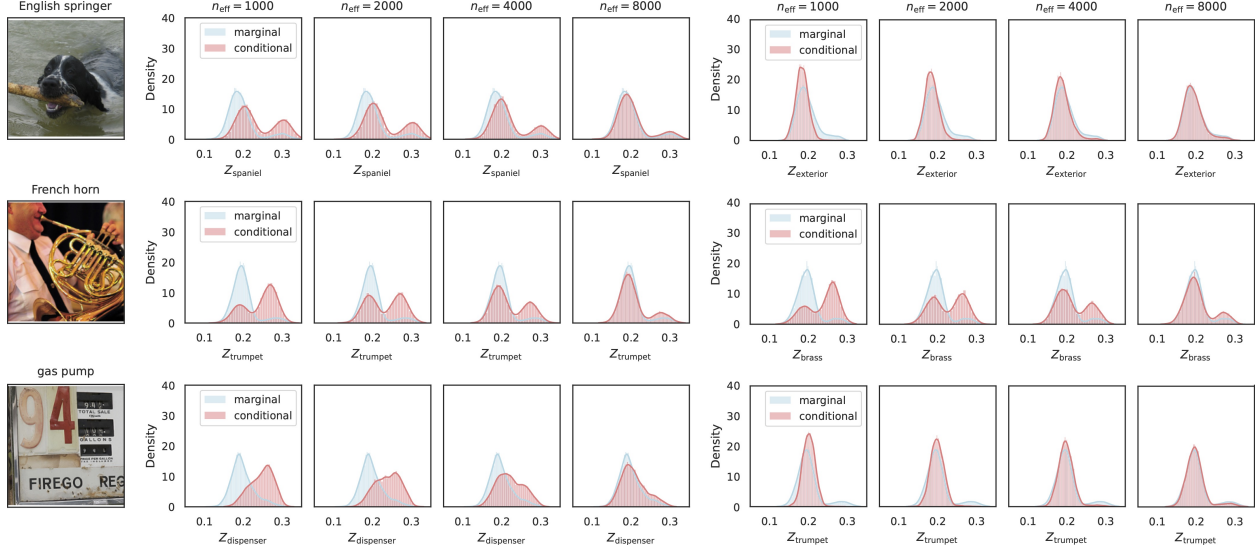


Figure D.1: Example marginal and estimated conditional distributions  $p(z_j)$  and  $\tilde{p}(z_j|z_{-j})$  for two class-specific concepts on three images from the Imagenette dataset. Distributions are shown as a function of the effective number of points in the weighted KDE (i.e.,  $n_{\text{eff}}$ ).

Fig. D.1 shows the marginal (i.e.,  $p(z_j)$ ) and estimated conditional distributions (i.e.,  $\tilde{p}(z_j|z_{-j})$ ) of two class-specific concepts as a function of effective number of points  $n_{\text{eff}}$  for three images in the Imagenette dataset. We can see how as  $n_{\text{eff}}$  increases, the estimated conditional distribution becomes closer to the marginal, and that the conditional distributions of class-specific concepts tend to be skewed to higher values compared to their marginals. This behavior suggests that images from a specific class have higher values of concepts that are related to the class. We use  $n_{\text{eff}} = 2000$  for all tests across all real-world experiments.

### D.1.2 Estimating $P_{H|Z_C=z_C}$ for x-SKIT

Here, we describe how to sample from the conditional distribution of dense embeddings  $H$  conditionally on any subset of concepts  $C \subseteq [m]$  of a particular semantic vector  $z \in [-1, 1]^m$ , i.e.  $\tilde{H}_C \sim P_{H|Z_C=z_C}$ , which is necessary to run our x-SKIT test. We show how to achieve this by coupling the nonparametric sampler introduced above with ideas of nearest neighbors. This choice is motivated by the need to keep samples in-distribution with respects to the downstream classifier  $g$ . Intuitively, we propose to:

1. Sample  $\tilde{Z} \sim P_{Z|Z_C=z_C}$ , and then
2. Retrieve the embedding  $H^{(i')}$  such that its concept representation  $Z^{(i')}$  is the nearest neighbor of  $\tilde{Z}$ .

Step 2. above makes sure that samples are coming from *real images*, and it overcomes some of the hurdles of sampling a high-dimensional vector ( $H \in \mathbb{R}^d$ ,  $d \sim 10^2$ ) conditionally on a low-dimensional one ( $z_C \in [-1, 1]^{|C|}$ ,  $C \subseteq [m]$ ,  $m \approx 20$ ). More precisely, recall that  $\{(h^{(i)}, z^{(i)})\}_{i=1}^n$  is a set of  $n$  pairs of dense embeddings and their semantics, then

$$\tilde{H}_C = h^{(i')} \quad \text{s.t.} \quad i' = \arg \min_{i \in [n]} \|z^{(i)} - \tilde{Z}\|, \quad \tilde{Z} \sim P_{Z|Z_C=z_C}, \quad (99)$$

where  $P_{Z|Z_C=z_C}$  is approximated with  $\tilde{p}(z_{-C} | z_C)$ ,  $-C := [m] \setminus C$  as in Eq. (97).

Fig. D.2 shows some example test (i.e.,  $g(\tilde{H}_{S \cup \{j\}})$ ) and null distributions (i.e.,  $g(\tilde{H}_S)$ ) for a class-specific concept and a non-class specific one on the same three images from the Imagenette dataset as in Fig. D.1.

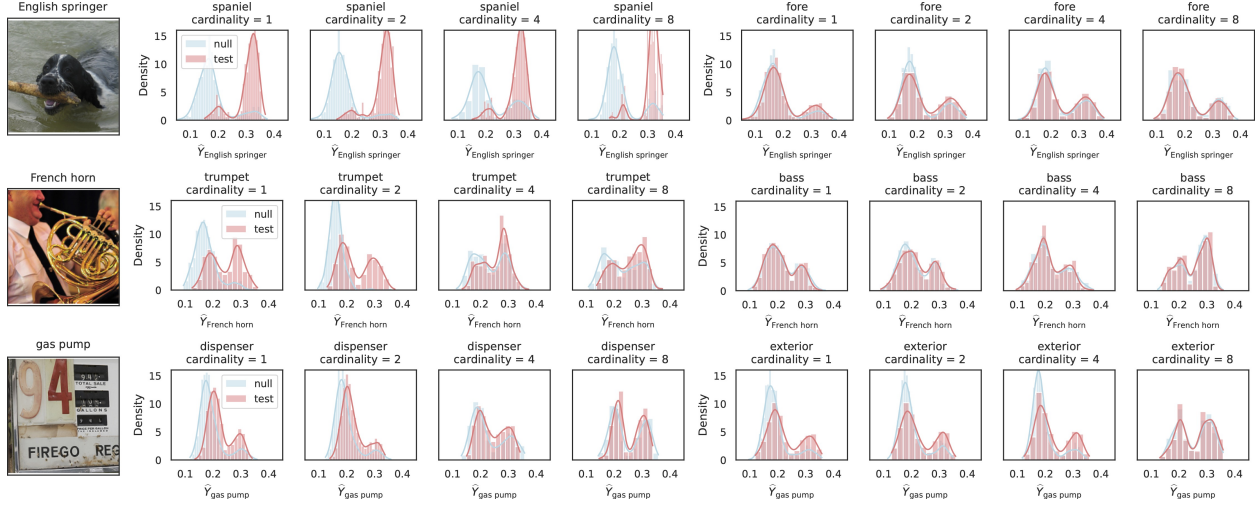


Figure D.2: Example test (i.e.,  $g(\tilde{H}_{S \cup \{j\}})$ ) and null (i.e.,  $g(\tilde{H}_S)$ ) distributions for a class-specific concept and a non-class specific one on three images from the Imagenette dataset as a function of the cardinality of  $S$ .

We remark that  $S$  can be any subset of the remaining concepts, so we show results for random subsets of increasing size. We can see that the test distributions of class-specific concepts are skewed to the right, i.e. including the observed class-specific concept increases the output of the predictor. Furthermore, we see the shift decreases the more concepts are included in  $S$ , i.e. if  $S$  is larger and it contains more information, then the marginal contribution of one additional concept will be smaller. On the other hand, including a non-class-specific concept does not change the distribution of the response of the model, no matter the size of  $S$ —precisely as our local definition of importance ( $H_{0,j,S}^{\text{LC}}$ ) demands.

## D.2 AwA2 Dataset

In this section, we include additional tables and figures for the AwA2 dataset experiment.



Figure D.3: Example images from the top-10 best classified classes in the AwA2 dataset.

Table D.1: Zero-shot classification accuracy on the AwA2 dataset.

Model	Accuracy									
	giant panda	tiger	giraffe	zebra	lion	squirrel	sheep	horse	elephant	dalmatian
CLIP-RN50	100.00%	100.00%	100.00%	100.00%	99.51%	99.17%	97.54%	98.18%	94.71%	96.36%
CLIP-ViT-B/32	100.00%	100.00%	100.00%	100.00%	99.51%	99.58%	98.59%	99.39%	99.04%	98.18%
CLIP-ViT-L/14	100.00%	100.00%	99.59%	100.00%	100.00%	100.00%	99.65%	98.78%	100.00%	100.00%
OpenClip-ViT-B-32	100.00%	100.00%	100.00%	100.00%	100.00%	99.58%	99.65%	98.78%	100.00%	97.27%
OpenClip-ViT-L-14	100.00%	100.00%	100.00%	100.00%	100.00%	100.00%	100.00%	100.00%	100.00%	100.00%
FLAVA	100.00%	98.86%	100.00%	100.00%	99.02%	99.17%	100.00%	99.39%	99.04%	98.18%
ALIGN	100.00%	100.00%	100.00%	99.57%	100.00%	99.58%	99.65%	99.70%	100.00%	99.09%
BLIP	100.00%	100.00%	99.17%	99.15%	99.51%	99.17%	98.94%	99.39%	100.00%	100.00%
average	100.00% $\pm$ 0.00	99.86% $\pm$ 0.38	99.84% $\pm$ 0.29	99.84% $\pm$ 0.30	99.69% $\pm$ 0.34	99.53% $\pm$ 0.33	99.25% $\pm$ 0.80	99.20% $\pm$ 0.55	99.10% $\pm$ 1.71	98.64% $\pm$ 1.29

Table D.2: Class-level attributes tested on the AwA2 dataset.

Class	Attributes (20)	
	present (10)	absent (10)
giant panda	patches, old world, furry, black, big, white, walks, paws, bulbous, vegetation	flies, flippers, hooves, desert, hairless, red, blue, horns, plankton, yellow
tiger	stripes, stalker, meat, meat teeth, hunter, strong, fierce, old world, muscle, big	strain teeth, tunnels, hops, plankton, bipedal, tusks, flippers, flies, small, skimmer
giraffe	long neck, long legs, big, quadrupedal, spots, vegetation, lean, old world, walks, ground	bipedal, hibernate, cave, mountains, ocean, hunter, water, stripes, gray, fish
zebra	stripes, old world, quadrupedal, black, white, ground, group, grazer, walks, hooves	blue, spots, brown, water, coastal, patches, tusks, claws, scavenger, red
lion	meat, stalker, strong, hunter, meat teeth, big, fierce, paws, furry, old world	tunnels, blue, horns, skimmer, long neck, water, flippers, tusks, arctic, spots
squirrel	tail, furry, forager, small, gray, tree, new world, forest, vegetation, brown	horns, blue, yellow, tusks, meat teeth, flippers, scavenger, desert, plankton, strain teeth
sheep	white, quadrupedal, walks, group, vegetation, grazer, ground, fields, furry, new world	arctic, flippers, insects, paws, long neck, red, yellow, swims, plankton, hands
horse	hooves, fast, grazer, big, long legs, tail, quadrupedal, fields, brown, strong	arctic, tree, bipedal, plankton, fish, stripes, ocean, strain teeth, scavenger, orange
elephant	big, old world, gray, tough skin, quadrupedal tusks, hairless, strong, ground, walks	claws, flippers, orange, swims, ocean stripes, tunnels, plankton, coastal, strain teeth
dalmatian	big, old world, gray, tough skin, quadrupedal tusks, hairless, strong, ground, walks	claws, flippers, orange, swims, ocean stripes, tunnels, plankton, coastal, strain teeth

Table D.3: Comparison of SKIT, c-SKIT, and PCBM on the AwA2 dataset for all models.

Model	Importance	Accuracy	$f_1$ score
CLIP-RN50	SKIT	98.55%	0.69
	c-SKIT	98.55%	0.58
	PCBM	94.35%	0.45
CLIP-ViT-B/32	SKIT	99.43%	0.75
	c-SKIT	99.43%	0.58
	PCBM	95.39%	0.48
CLIP-ViT-L/14	SKIT	99.80%	0.75
	c-SKIT	99.80%	0.58
	PCBM	94.81%	0.52
OpenClip-ViT-B-32	SKIT	99.53%	0.55
	c-SKIT	99.53%	0.56
	PCBM	93.84%	0.53
OpenClip-ViT-L-14	SKIT	100.0%	0.57
	c-SKIT	100.0%	0.54
	PCBM	95.87%	0.50
FLAVA	SKIT	99.37%	0.61
	c-SKIT	99.37%	0.59
	PCBM	96.08%	0.48
ALIGN	SKIT	99.76%	0.62
	c-SKIT	99.76%	0.53
	PCBM	96.45%	0.42
BLIP	SKIT	99.53%	0.69
	c-SKIT	99.53%	0.62
	PCBM	93.85%	0.54

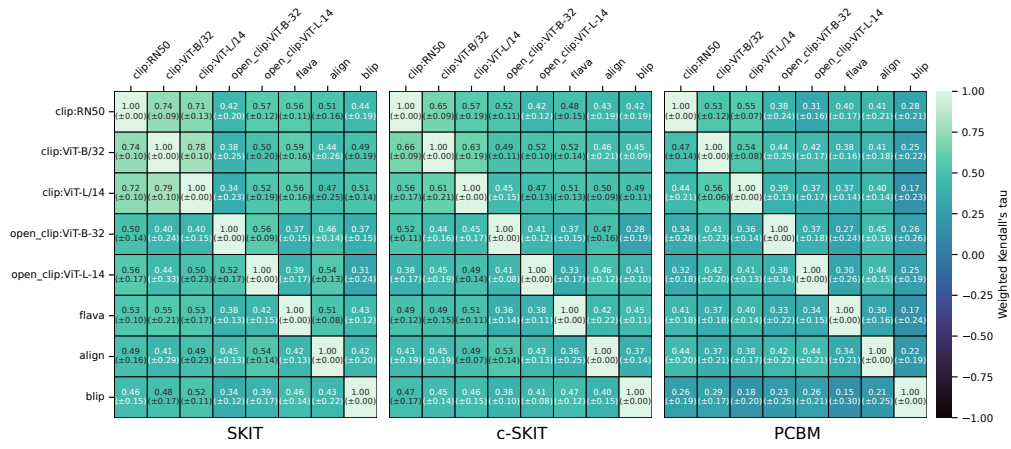


Figure D.4: Rank agreement comparison between SKIT, c-SKIT, and PCBM on the AwA2 dataset across 8 different vision-language models. Results are reported as mean and standard deviation over the 10 classes considered in this experiment.

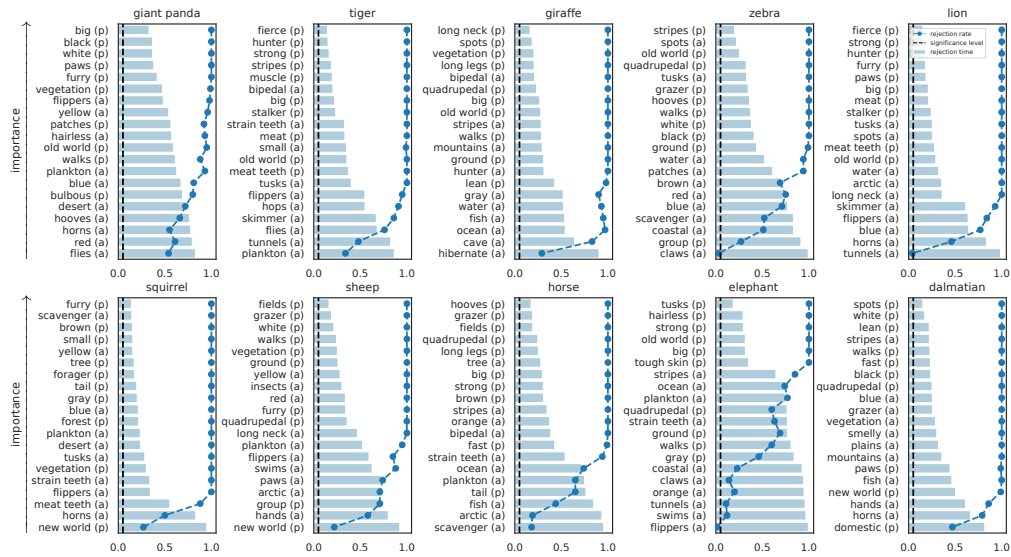


Figure D.5: SKIT importance results for CLIP:ViT-L/14 on the AwA2 dataset.

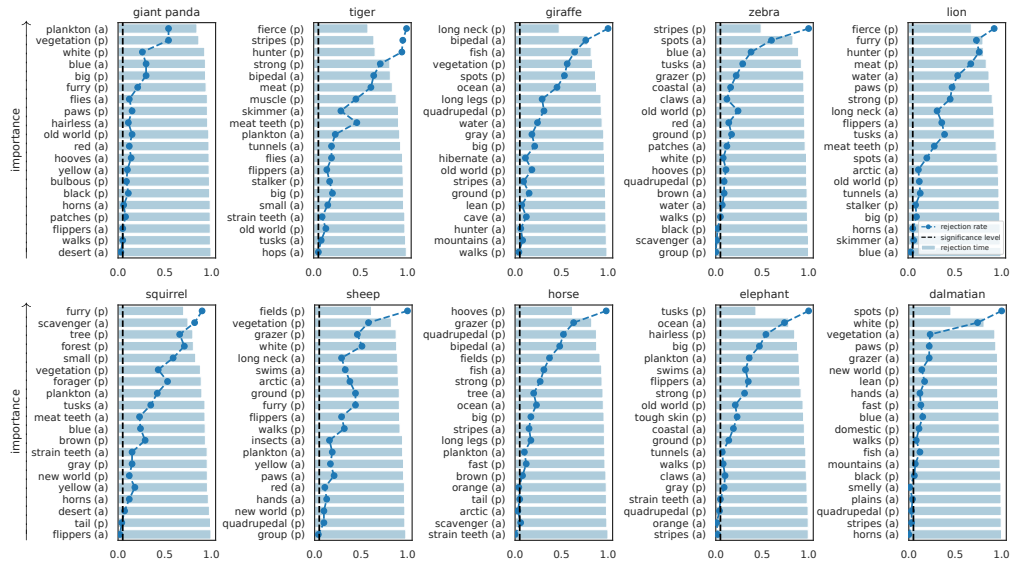


Figure D.6: c-SKIT importance results for CLIP:ViT-L/14 on the AwA2 dataset.



### D.3 CUB Dataset

In this section, we include additional tables and figures for the CUB dataset experiment.

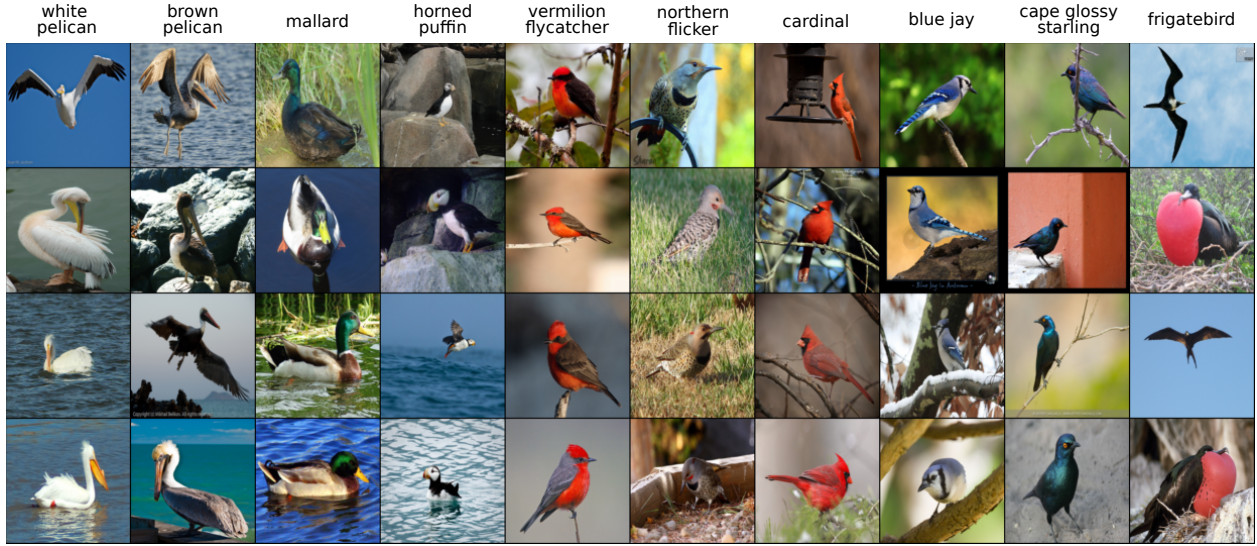


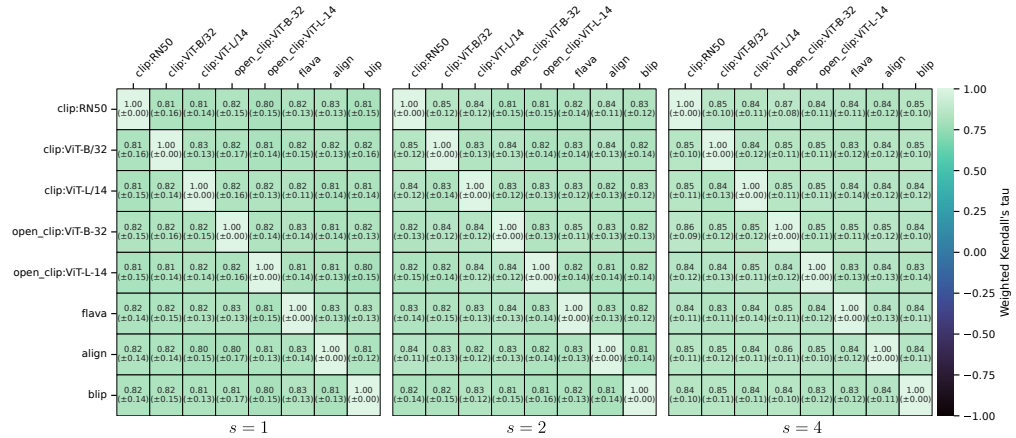
Figure D.7: Example test images from the CUB dataset with their respective classes.

Table D.4: Zero-shot classification accuracy on the CUB dataset.

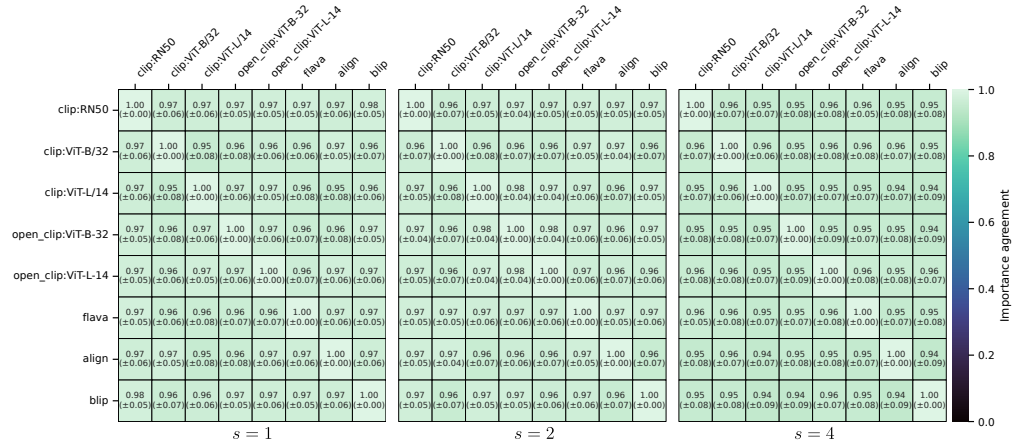
Model	Accuracy									
	white pelican	brown pelican	mallard	horned puffin	vermilion flycatcher	northern flicker	cardinal	blue jay	cape glossy starling	frigatebird
CLIP-RN50	92.00%	95.00%	95.00%	86.67%	88.33%	78.33%	63.16%	65.00%	73.33%	78.33%
CLIP-ViT-B/32	98.00%	96.67%	90.00%	93.33%	93.33%	98.33%	71.93%	83.33%	90.00%	80.00%
CLIP-ViT-L/14	98.00%	100.00%	100.00%	95.00%	100.00%	98.33%	100.00%	85.00%	100.00%	96.67%
OpenClip-ViT-B-32	100.00%	98.33%	98.33%	88.33%	96.67%	96.67%	100.00%	88.33%	96.67%	88.33%
OpenClip-ViT-L-14	100.00%	100.00%	100.00%	96.67%	100.00%	100.00%	100.00%	91.67%	95.00%	93.33%
FLAVA	100.00%	100.00%	98.33%	95.00%	91.67%	76.67%	100.00%	91.67%	88.33%	90.00%
ALIGN	96.00%	96.67%	95.00%	98.33%	78.33%	86.67%	92.98%	83.33%	80.00%	55.00%
BLIP	98.00%	80.00%	96.67%	65.00%	55.00%	61.67%	61.40%	90.00%	73.33%	75.00%
average	97.75% $\pm$ 2.54%	95.83% $\pm$ 6.24%	96.67% $\pm$ 3.12%	89.79% $\pm$ 10.08%	87.92% $\pm$ 14.09%	87.08% $\pm$ 12.96%	86.18% $\pm$ 16.42%	84.79% $\pm$ 8.14%	87.08% $\pm$ 9.75%	82.08% $\pm$ 12.47%

Table D.5: x-SKIT importance detection  $f_1$  score on the CUB dataset as a function of conditioning set size  $s$  for all models used in the experiment.

Model	Importance $f_1$ score			Model	Importance $f_1$ score		
	$s = 1$	$s = 2$	$s = 4$		$s = 1$	$s = 2$	$s = 4$
CLIP-RN50	0.92 $\pm$ 0.15	0.91 $\pm$ 0.15	0.88 $\pm$ 0.17	OpenClip-ViT-L-14	0.94 $\pm$ 0.13	0.92 $\pm$ 0.16	0.88 $\pm$ 0.16
CLIP-ViT-B/32	0.93 $\pm$ 0.14	0.95 $\pm$ 0.09	0.90 $\pm$ 0.13	FLAVA	0.93 $\pm$ 0.13	0.93 $\pm$ 0.13	0.89 $\pm$ 0.15
CLIP-ViT-L/14	0.92 $\pm$ 0.16	0.92 $\pm$ 0.16	0.88 $\pm$ 0.15	ALIGN	0.95 $\pm$ 0.13	0.94 $\pm$ 0.12	0.91 $\pm$ 0.11
OpenClip-ViT-B-32	0.91 $\pm$ 0.17	0.92 $\pm$ 0.15	0.89 $\pm$ 0.14	BLIP	0.92 $\pm$ 0.15	0.91 $\pm$ 0.17	0.86 $\pm$ 0.19



(a) Rank agreement.



(b) Importance agreement.

Figure D.8: x-SKIT agreement results on the CUB dataset across 8 different vision-language models as a function of conditioning set size,  $s$ . Results are reported as means and standard deviations over the random 100 images used in the experiment.

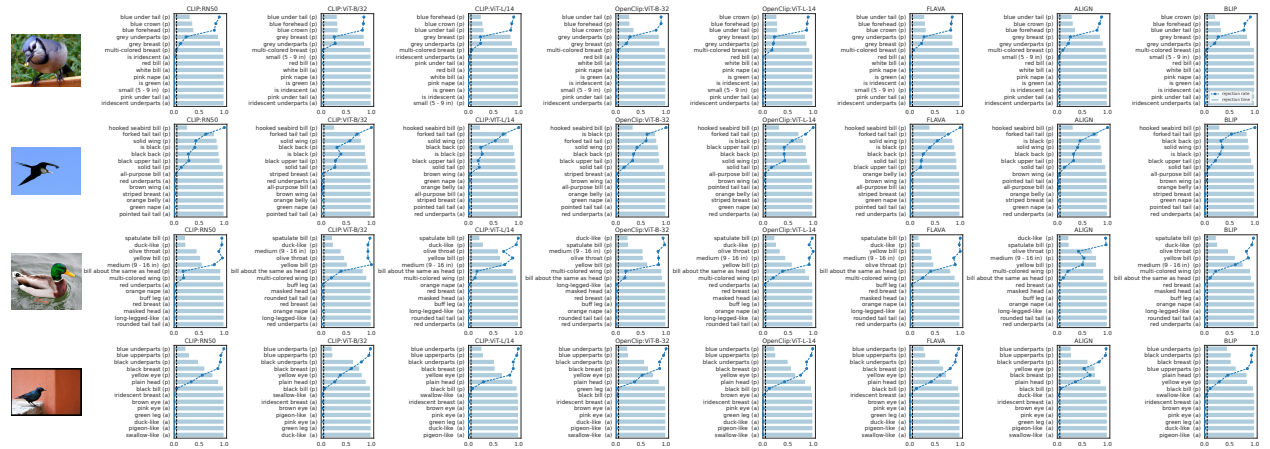


Figure D.9: x-SKIT ranks of importance across all models for four example images in the CUB dataset. Results are averaged over 100 repetitions of the tests with  $\tau^{\max} = 200$ , and conditioning on random subsets of 1 concept (i.e.,  $s = 1$ ).



## D.4 Imagenette Dataset

In this section, we include additional tables and figures for the Imagenette dataset experiment.

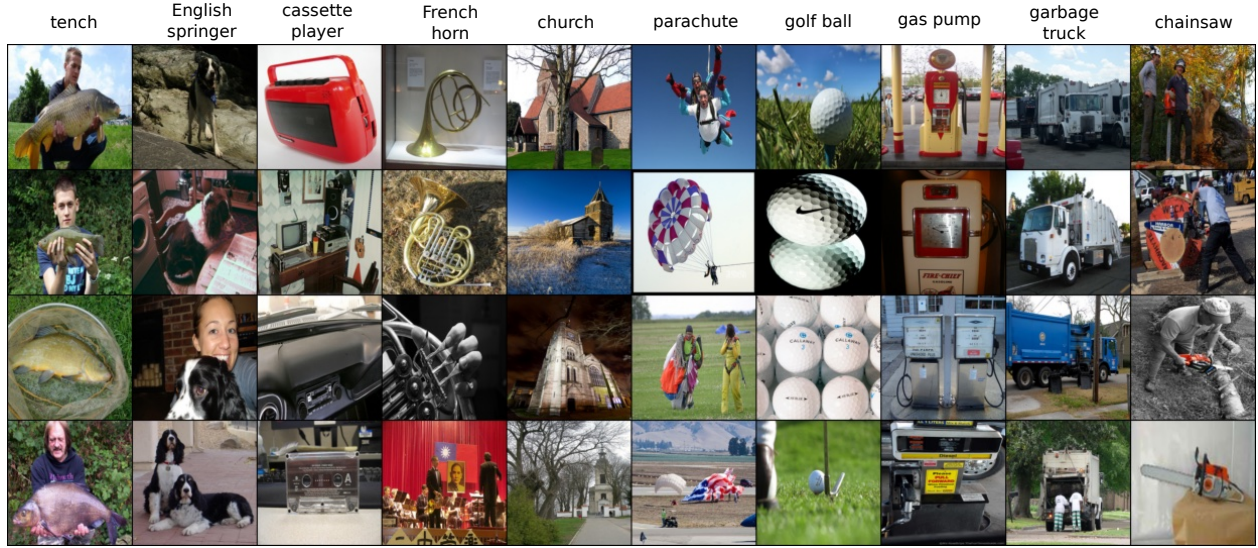


Figure D.10: Example images from the Imagenette dataset with their respective labels.

Table D.6: Zero-shot classification accuracy on the Imagenette dataset.

Model	Accuracy									
	tench	English springer	cassette player	French horn	church	parachute	golf ball	gas pump	garbage truck	chainsaw
CLIP-RN50	99.48%	99.49%	95.80%	99.49%	100.00%	99.74%	97.74%	91.65%	98.71%	96.63%
CLIP-ViT-B/32	99.74%	99.24%	96.08%	98.73%	100.00%	98.97%	99.25%	97.61%	99.49%	99.22%
CLIP-ViT-L/14	99.22%	99.75%	99.72%	99.75%	100.00%	99.74%	99.75%	100.00%	99.74%	99.74%
OpenClip-ViT-B-32	100.00%	100.00%	98.32%	99.24%	99.76%	99.49%	99.25%	97.61%	99.23%	97.67%
OpenClip-ViT-L-14	100.00%	100.00%	99.72%	99.75%	100.00%	100.00%	99.50%	99.28%	99.49%	98.96%
FLAVA	99.74%	99.24%	97.76%	98.22%	100.00%	98.72%	99.00%	97.61%	99.23%	96.37%
ALIGN	99.74%	100.00%	99.44%	99.75%	100.00%	99.49%	99.75%	99.28%	99.49%	98.96%
BLIP	100.00%	98.48%	93.56%	99.75%	100.00%	99.49%	99.50%	98.09%	99.23%	98.19%
average	99.74% $\pm$ 0.26%	99.53% $\pm$ 0.50%	97.55% $\pm$ 2.09%	99.33% $\pm$ 0.54%	99.97% $\pm$ 0.08%	99.46% $\pm$ 0.39%	99.22% $\pm$ 0.61%	97.64% $\pm$ 2.43%	99.33% $\pm$ 0.29%	98.22% $\pm$ 1.15%

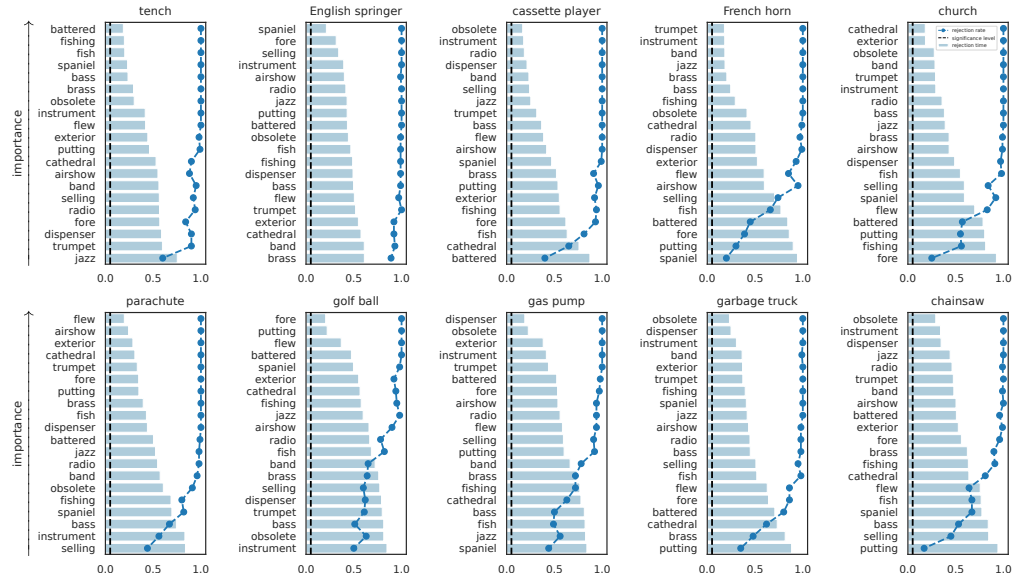


Figure D.11: SKIT importance results for CLIP-ViT-L/14 on the Imagenette dataset.

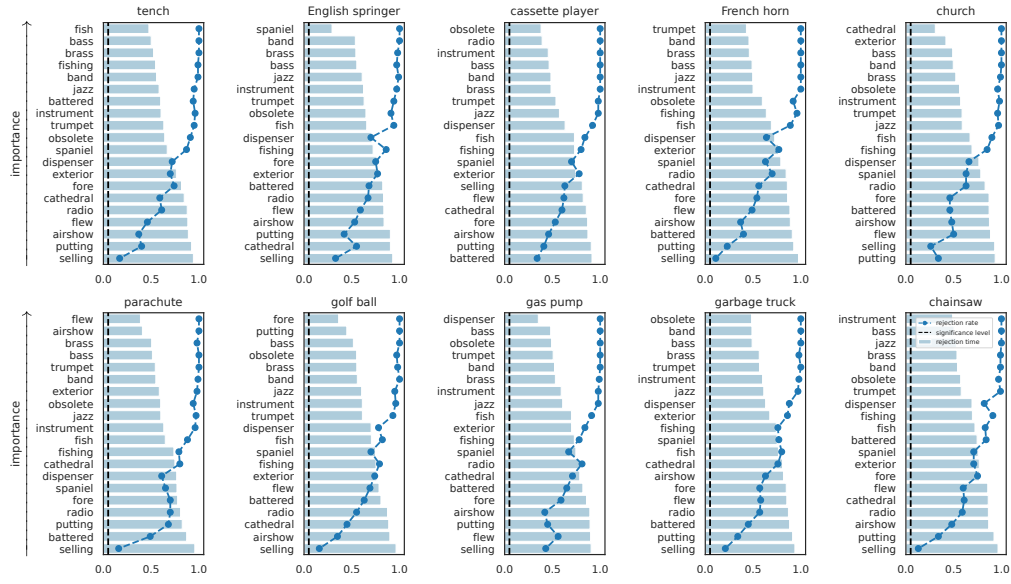


Figure D.12: c-SKIT importance results for CLIP:ViT-L/14 on the Imagenette dataset.

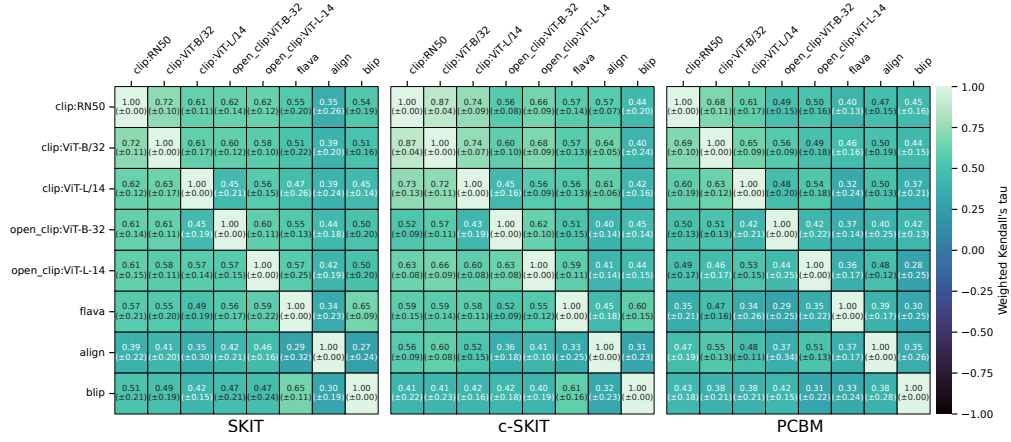


Figure D.13: Rank agreement comparison between SKIT, c-SKIT, and PCBM on the Imagenette dataset across 8 different vision-language models. Result are reported as mean and standard deviation over the 10 classes considered in the experiment.

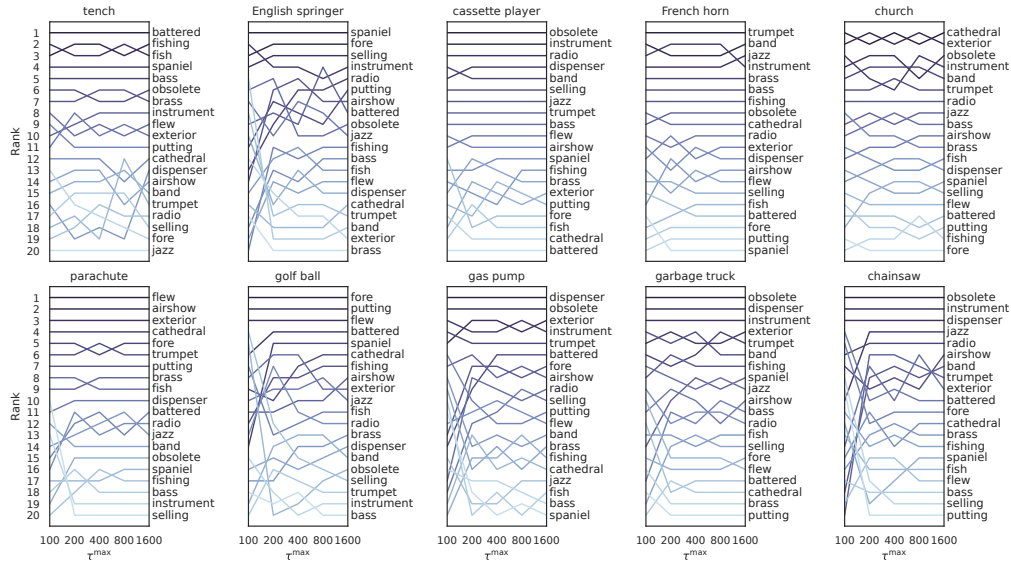


Figure D.14: SKIT ranks of importance for CLIP:ViT-L/14 on the Imagenette dataset as a function of  $\tau^{\max}$ .

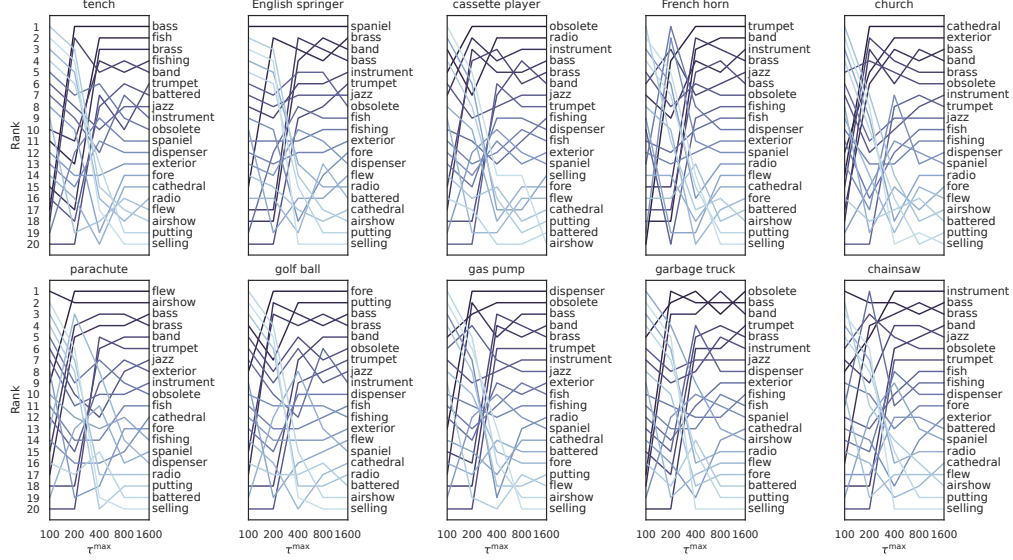
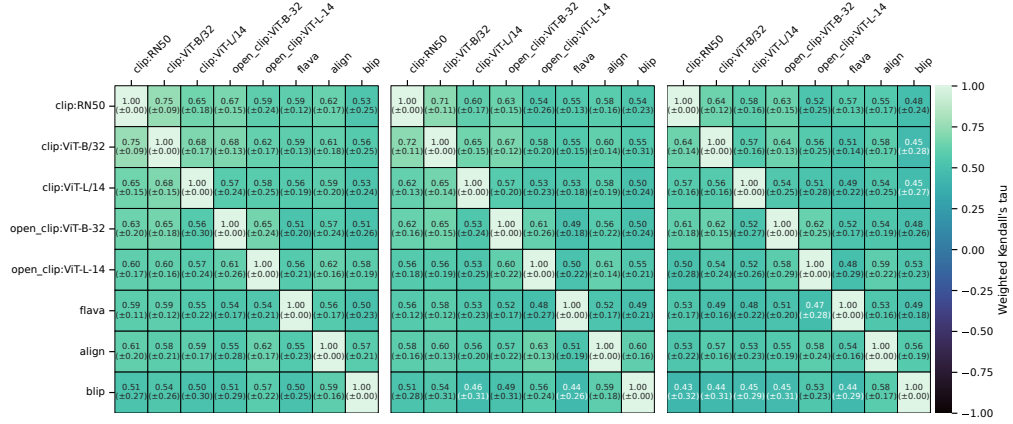
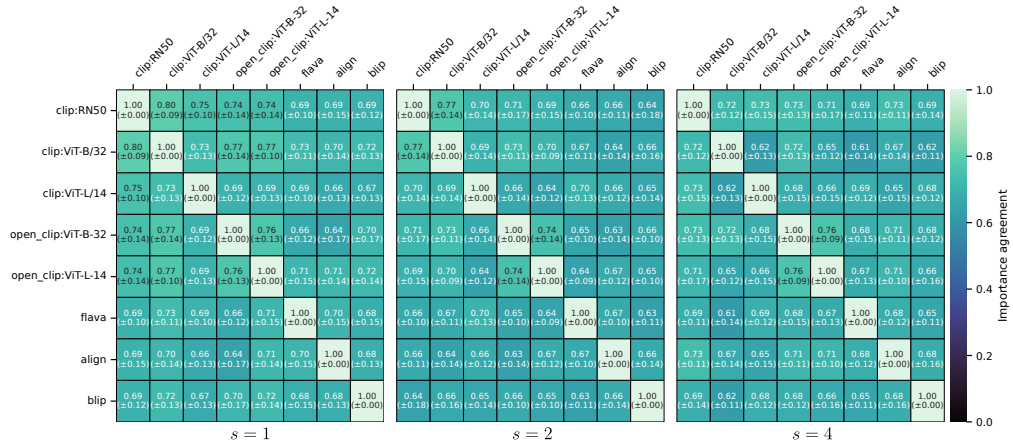


Figure D.15: c-SKIT ranks of importance for CLIP:ViT-L/14 on the Imagenette dataset as a function of  $\tau^{\max}$ .



(a) Rank agreement.



(b) Importance agreement.

Figure D.16: x-SKIT agreement results on the Imagenette dataset across 8 different vision-language models as a function of conditioning set size,  $s$ . Results are reported as means and standard deviations over the random 20 images used in the experiment.





Figure D.17: x-SKIT ranks of importance across all models for 2 examples images from 3 classes in the Imagenette dataset. Results are averaged over 100 repetitions of the tests with  $\tau^{\max} = 200$ , and conditioning on random subsets of 1 concept (i.e.,  $s = 1$ ).

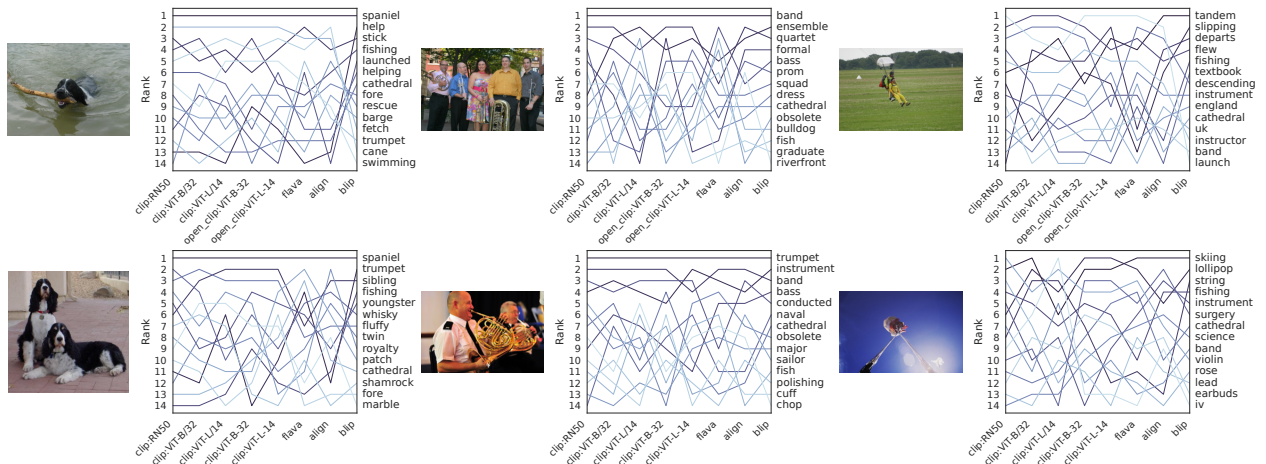


Figure D.18: Summary of x-SKIT ranks of importance across all models for 2 examples images from 3 classes in the Imagenette dataset.